MAGNETISM IN MATERIALS

Lecture 11: Experimental Techniques
NMR & μSR

Ivica Zivkovic

13.05.2025

EXPERIMENTAL TECHNIQUES

- NMR
- μSR

❖ medicine, chemistry, physics,…different needs, different approaches

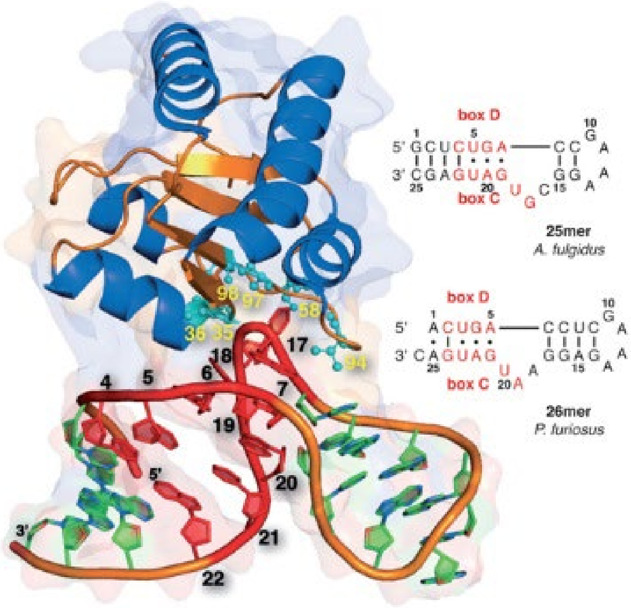

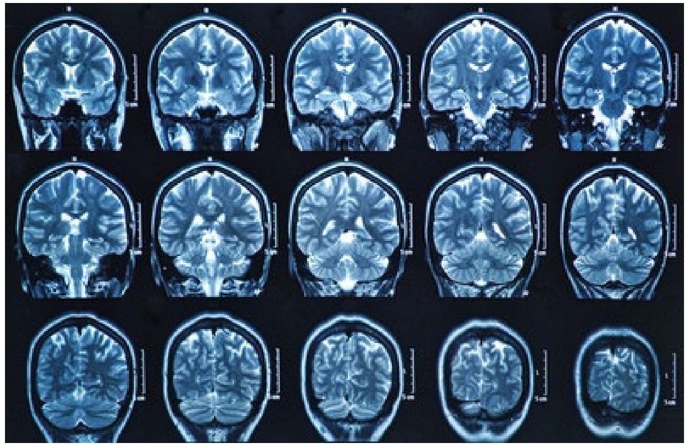

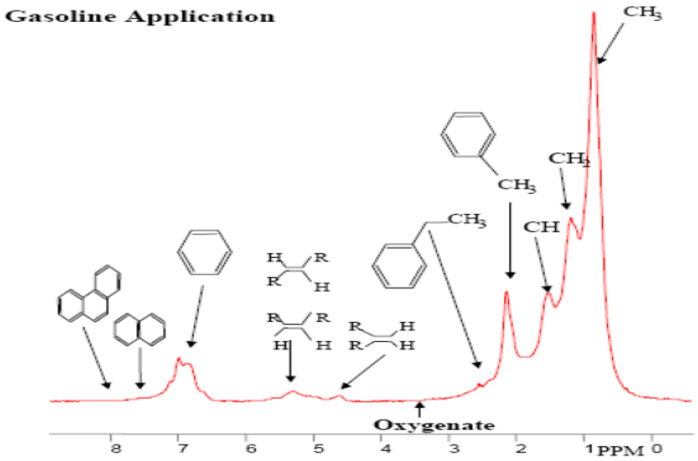

image source: wikimedia.org

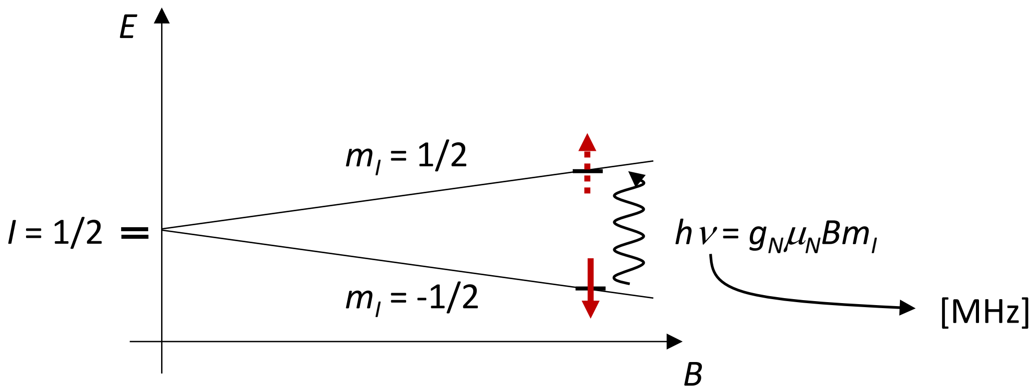

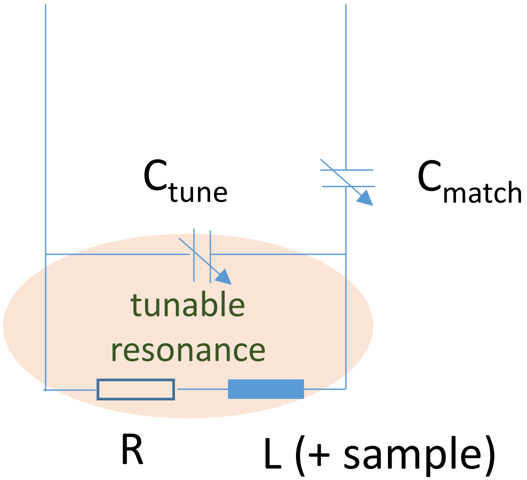

$$\mu_N = \frac{e\hbar}{2m_P} = 5.0508 \times 10^{-27}\,\mathrm{Am}^2$$

$$\mu = g_I \mu_N I$$

$$I_p = I_n = \frac{1}{2}$$

$$g_p = 5.586$$

$$g_n = -3.826$$

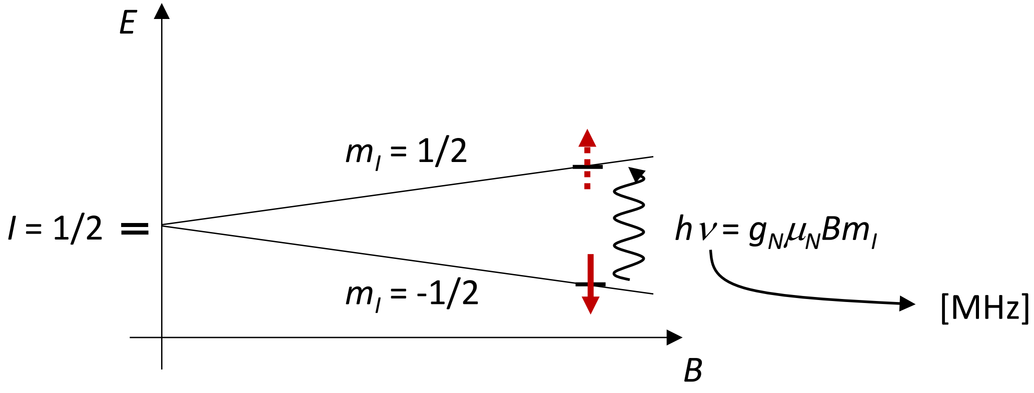

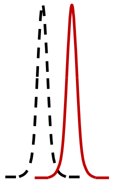

gyromagnetic ratio (1 – 40 MHz/T)

$$\nu_{NMR} = \frac{\gamma}{2\pi}(B + \delta B_{local})$$

in the limit of (ultra) weak coupling, the nucleus serves as a local magnetometer

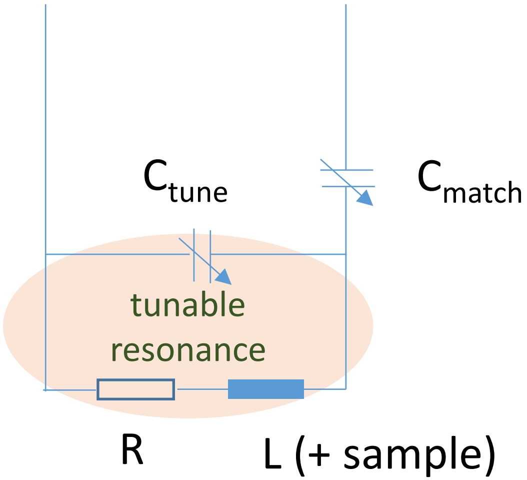

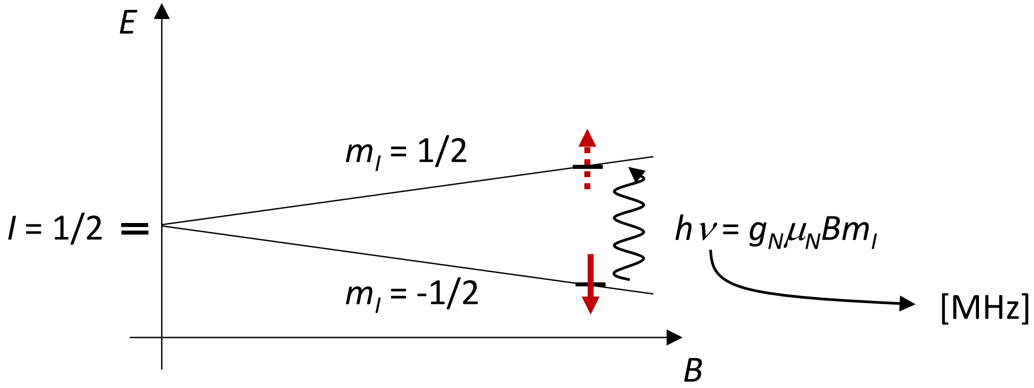

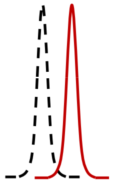

gyromagnetic ratio (1 – 40 MHz/T)

$$\nu_{NMR} = \frac{\gamma}{2\pi}(B + \delta B_{local})$$

in the limit of (ultra) weak coupling, the nucleus serves as a local magnetometer

PRB 69, 144404 (2004)

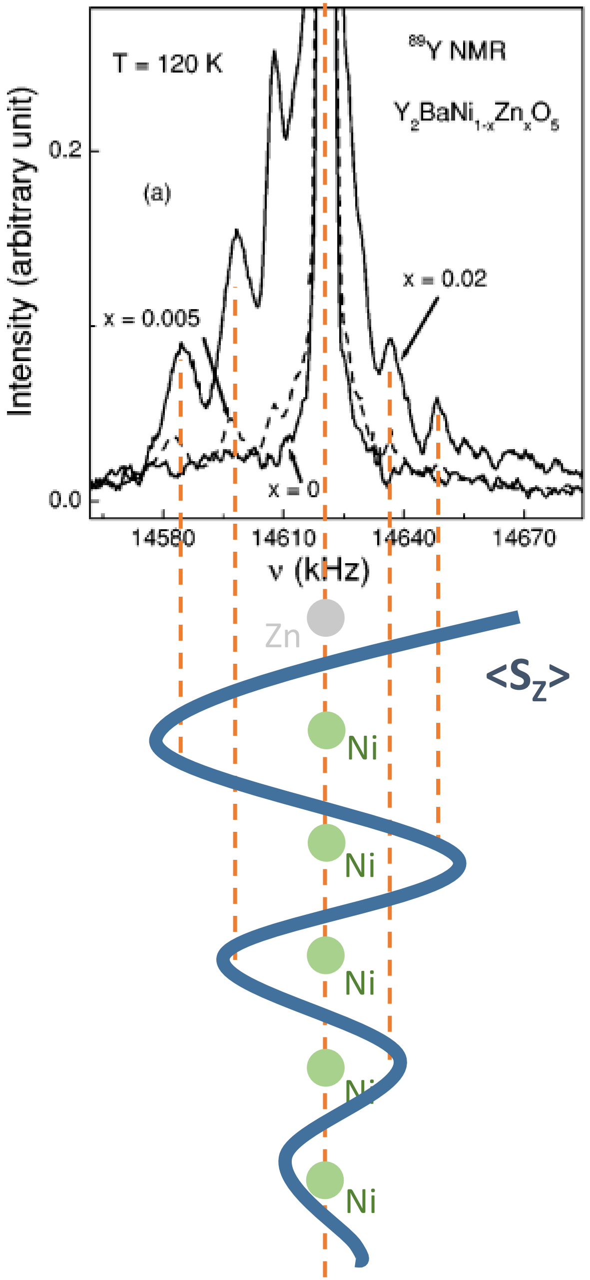

❖ NMR-active nuclei

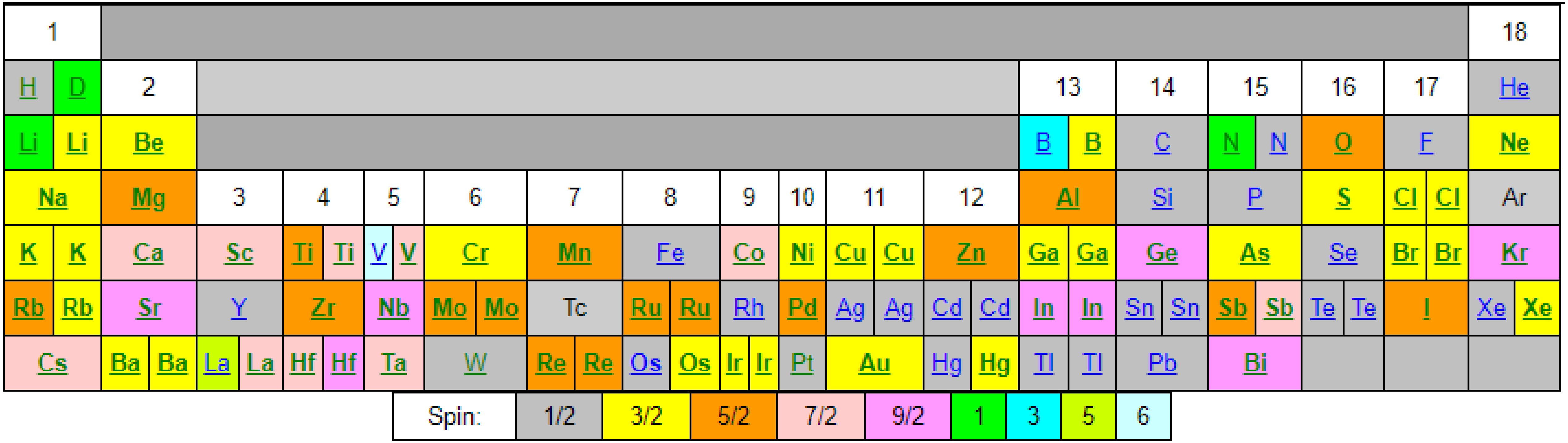

pascal-man.com

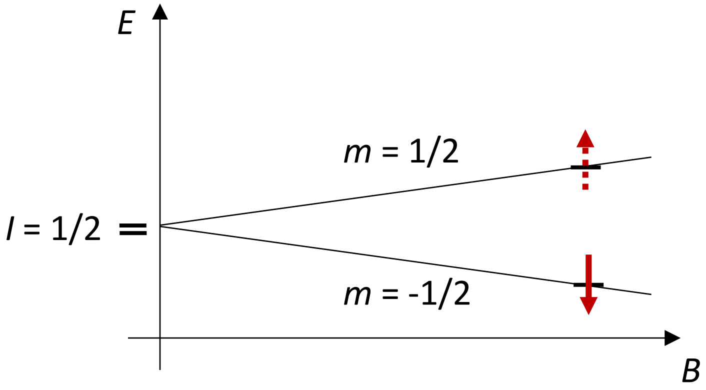

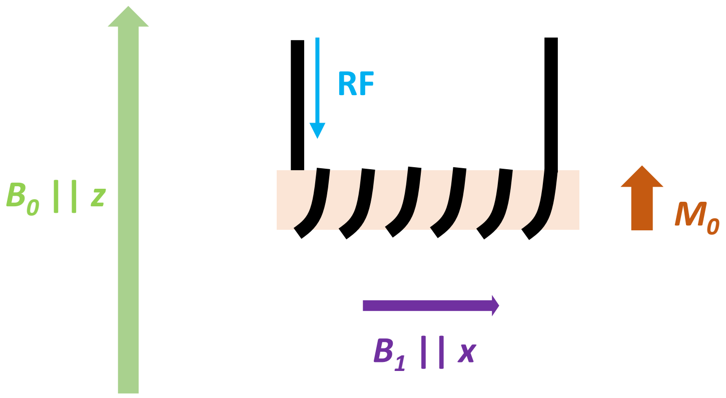

$$t_P = \frac{\pi}{2}(\omega_1)^{-1}$$

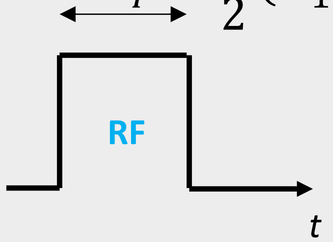

M_0 rotates from || z to || y ("$\pi/2$ – pulse")

$$\omega_1 = \gamma B_1$$

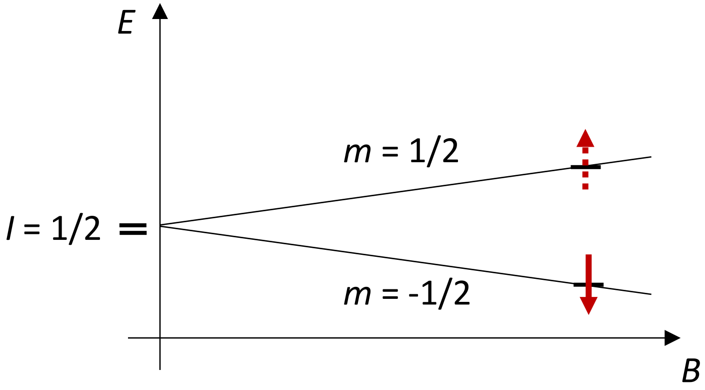

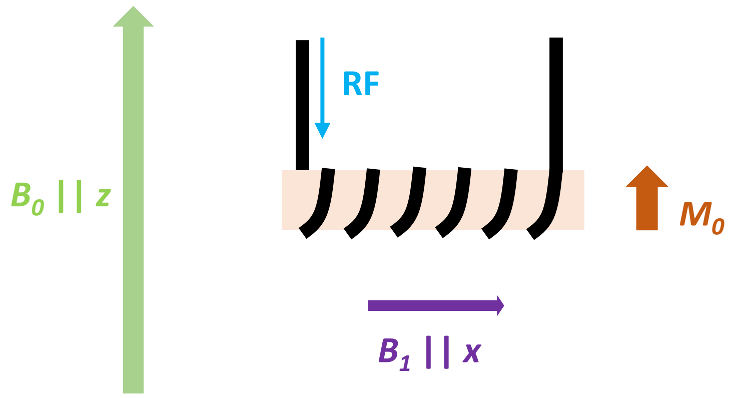

$$t_P = \frac{\pi}{2}(\omega_1)^{-1}$$

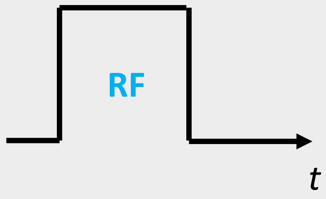

M_0 rotates from
|| z to || y
(“$\pi/2-$pulse”)

$$\omega_1 = \gamma B_1$$

two independent relaxation processes

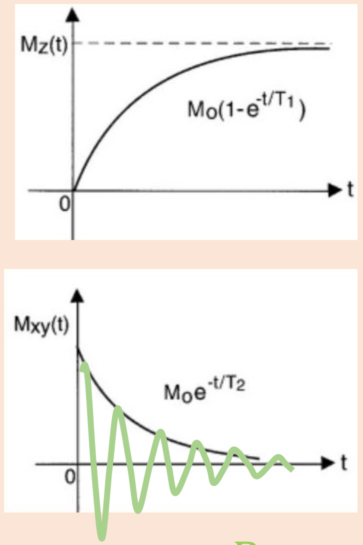

$$\omega_0 = \gamma B_0$$

free induction decay

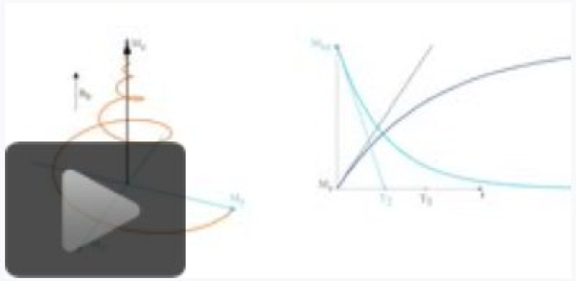

Visualization of the T_1 and T_2 relaxation times.

[T1/T2 relaxation]

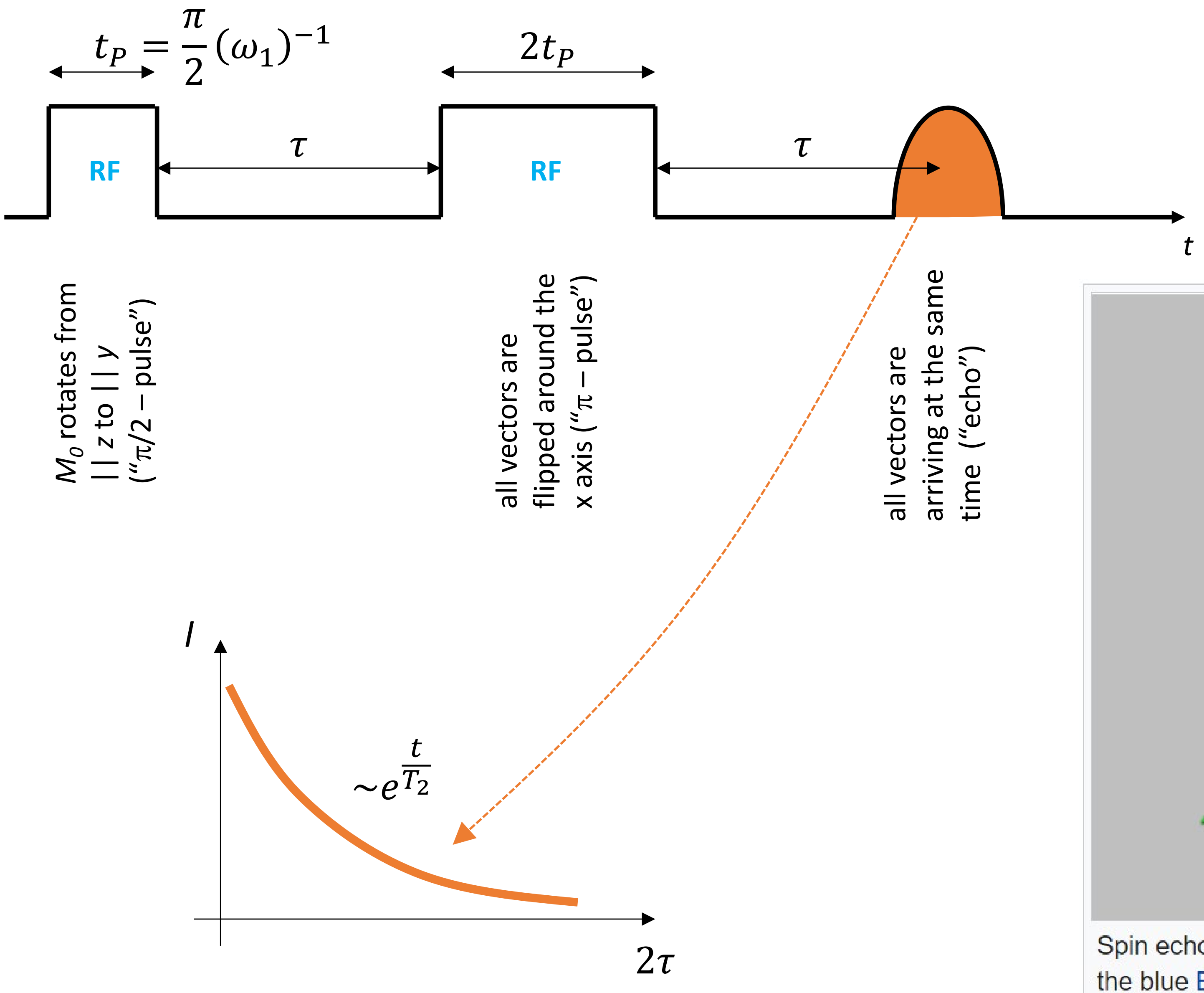

π/2-π-echo

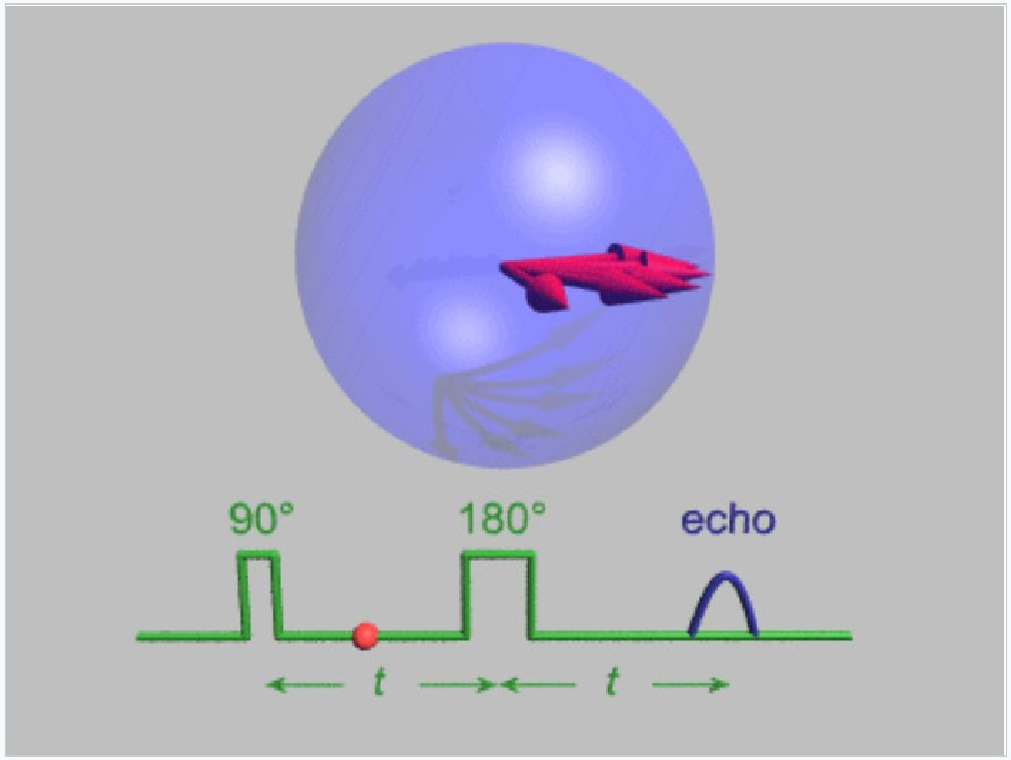

Spin echo animation showing the response of spins (red arrows) in the blue Bloch sphere to the green pulse sequence

$$\mathcal{H} = \mathcal{H}_n + \mathcal{H}_{n-n} + \mathcal{H}_{hf} + \mathcal{H}_{EFG}$$

electric-field gradient (charge distribution)

hyperfine interaction (multiple contributions)

indirect interaction between nuclear moments by electrons (usually safe to ignore)

Zeeman splitting (B_0 + screening of electrons in specific orbitals $\rightarrow$ chemical shift)

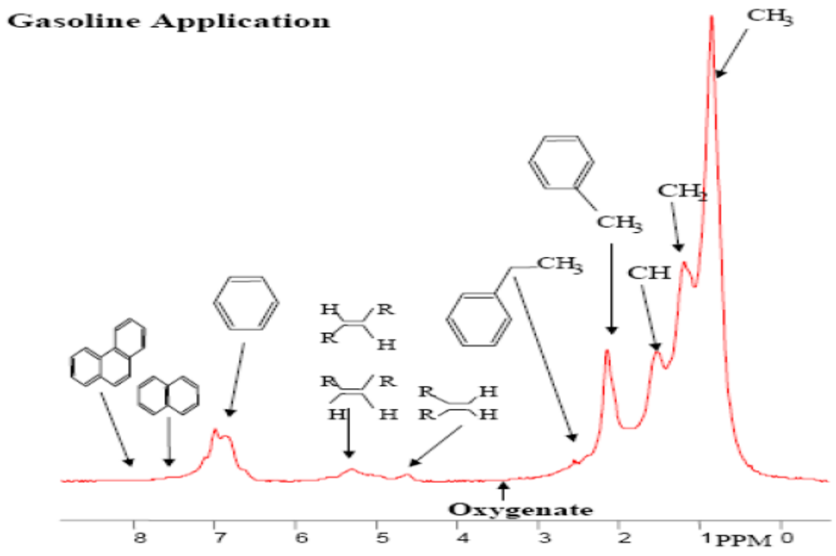

$$\mathcal{H} = \mathcal{H}_n + \mathcal{H}_{n-n} + \mathcal{H}_{hf} + \mathcal{H}_{EFG}$$

$\mathcal{H}_{EFG}$: electric-field gradient (charge distribution)

$\mathcal{H}_{hf}$: hyperfine interaction (multiple contributions)

$\mathcal{H}_{n-n}$: indirect interaction between nuclear moments by electrons (usually safe to ignore)

$\mathcal{H}_n$: Zeeman splitting (B_0 + screening of electrons in specific orbitals $\rightarrow$ chemical shift)

$$\mathcal{H}_{hf} = \underbrace{-\hbar^2\gamma_n\gamma_e\frac{\boldsymbol{I}\cdot\boldsymbol{L}}{r^3}}_{\text{orbital effect}} \underbrace{- \hbar^2\gamma_n\gamma_e\left[\frac{\boldsymbol{I}\cdot\boldsymbol{S}}{r^3} - 3\frac{(\boldsymbol{I}\cdot\boldsymbol{r})(\boldsymbol{S}\cdot\boldsymbol{r})}{r^5}\right]}_{\text{dipolar effect}} + \underbrace{\hbar^2\gamma_n\gamma_e\frac{8\pi}{3}\boldsymbol{I}\cdot\boldsymbol{S}\delta(r)}_{\text{Fermi contact}}$$

$\delta(r)$ → wave-function overlap (*s*-orbitals, metals)

$$\mathcal{H}_{EFG} = \frac{eQV_{zz}}{4I(2I-1)}\left[3I_z^2 - I(I+1) + \frac{\eta}{2}\left(I_x^2 - I_y^2\right)\right]$$

$$\eta = \frac{V_{xx} - V_{yy}}{V_{zz}} \qquad V_{\alpha\alpha} = \frac{\partial^2 V}{\partial \alpha^2}$$

$$eQ = \frac{1}{2}\int (3z^2 - r^2)\rho d^3r$$

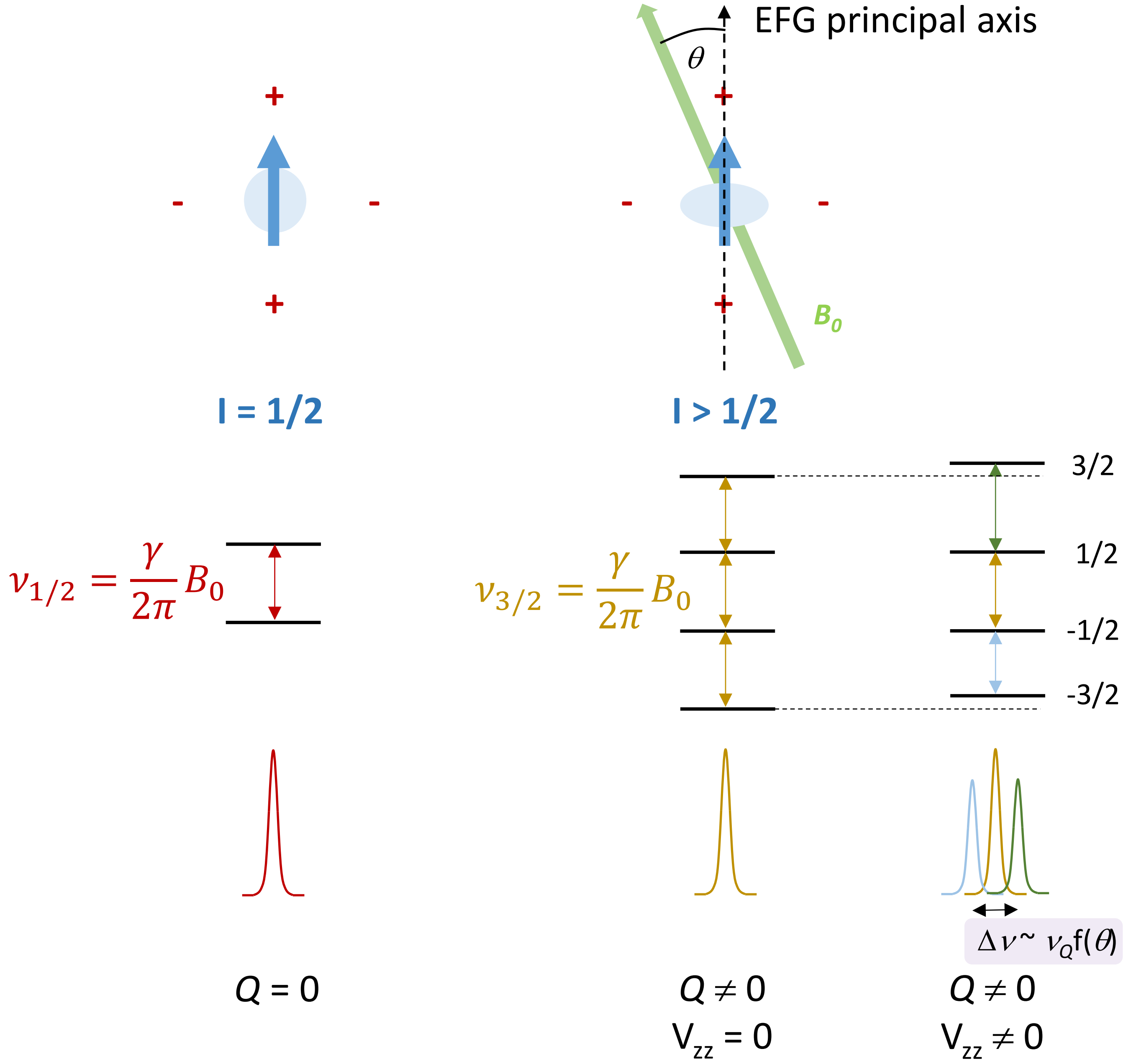

$$\mathcal{H}_{EFG} = \frac{eQV_{zz}}{4I(2I-1)}\left[3I_z^2 - I(I+1) + \frac{\eta}{2}\left(I_x^2 - I_y^2\right)\right]$$

$$\eta = \frac{V_{xx} - V_{yy}}{V_{zz}} \qquad V_{\alpha\alpha} = \frac{\partial^2 V}{\partial \alpha^2}$$

$$eQ = \frac{1}{2}\int (3z^2 - r^2)\rho d^3r$$

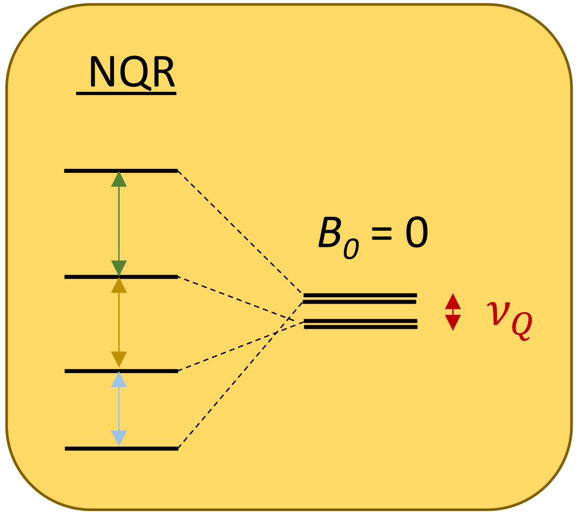

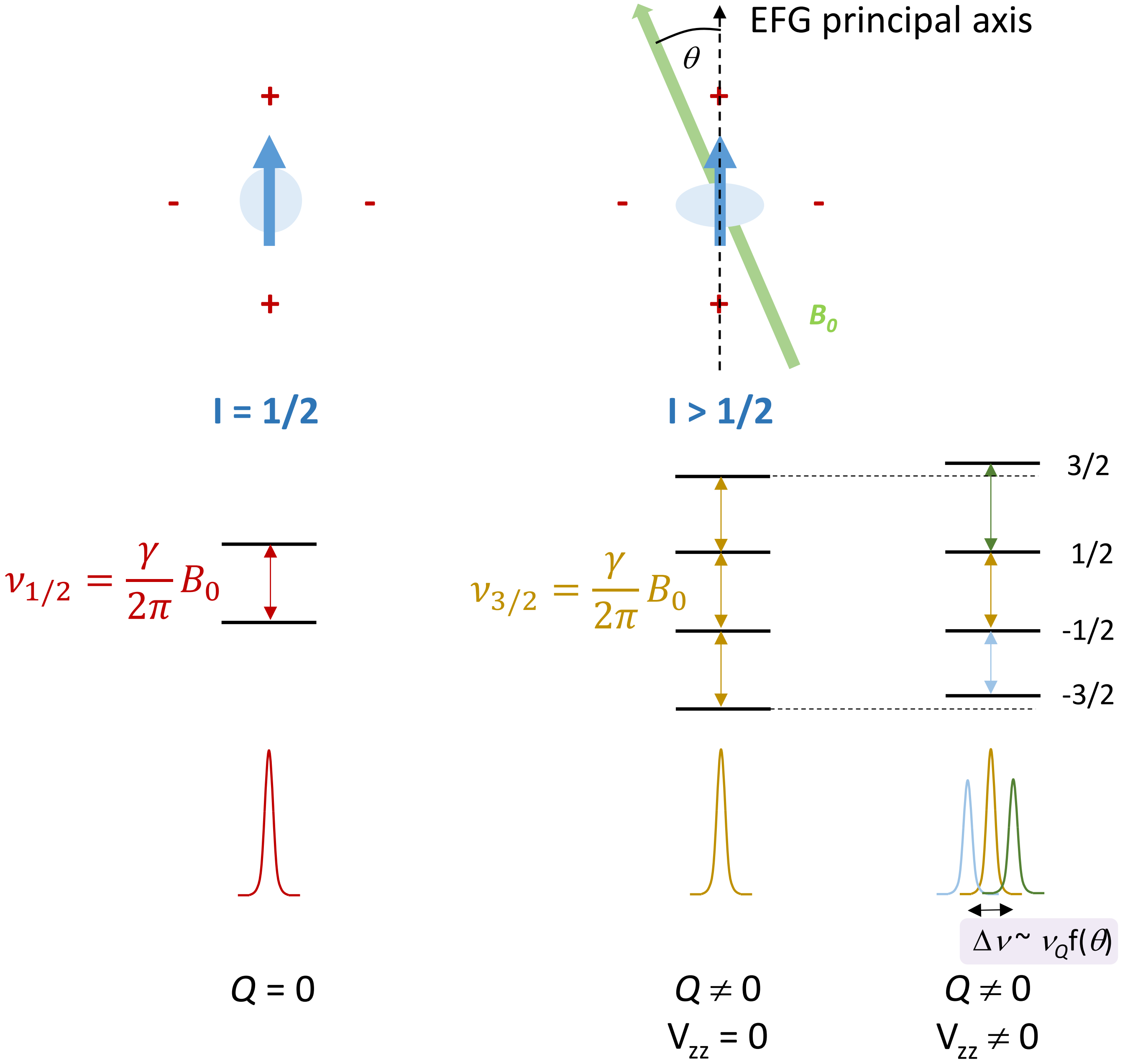

$$\mathcal{H}_{EFG} = \frac{eQV_{zz}}{4I(2I-1)}\left[3I_z^2 - I(I+1) + \frac{\eta}{2}\left(I_x^2 - I_y^2\right)\right]$$

$$\eta = \frac{V_{xx} - V_{yy}}{V_{zz}} \qquad V_{\alpha\alpha} = \frac{\partial^2 V}{\partial \alpha^2}$$

$$eQ = \frac{1}{2}\int (3z^2 - r^2)\rho d^3 r$$

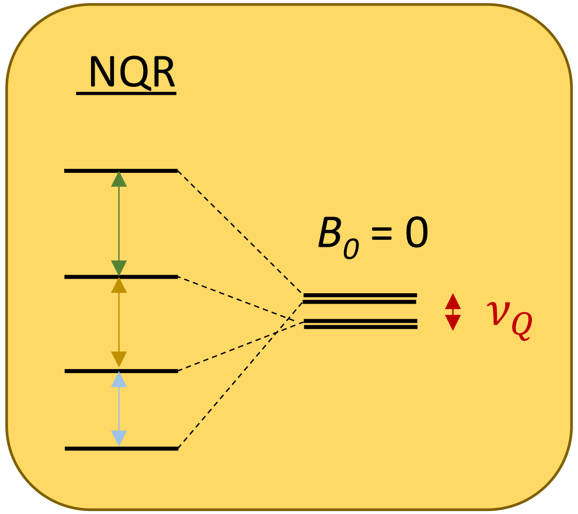

Journal of the Physical Society of Japan **92**, 034702 (2023)
https://doi.org/10.7566/JPSJ.92.034702

Editors' Choice

Symmetry Analysis of Zero-Field Antiferroquadrupole Order in CeB_6: Extremely Low-Frequency ^{11}B-NQR Study

Takeshi Mito[1*], Hiroki Mori[1], Keisuke Miyamoto[1], Taichi Tanaka[1], Yusuke Nakai[1], Koichi Ueda[1], Fumitoshi Iga[2], and Hisatomo Harima[3]

[1]*Department of Material Science, Graduate School of Science, University of Hyogo, Kamigori, Hyogo 678-1297, Japan*
[2]*Institute of Quantum Beam Science, Graduate School of Science and Engineering, Ibaraki University, Mito 310-8512, Japan*
[3]*Department of Physics, Graduate School of Science, Kobe University, Kobe 657-8501, Japan*

(Received September 2, 2022; accepted December 28, 2022; published online February 7, 2023)

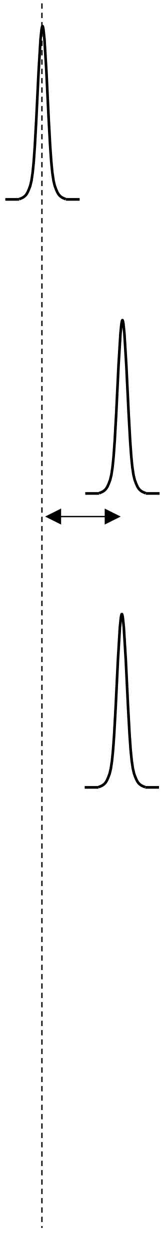

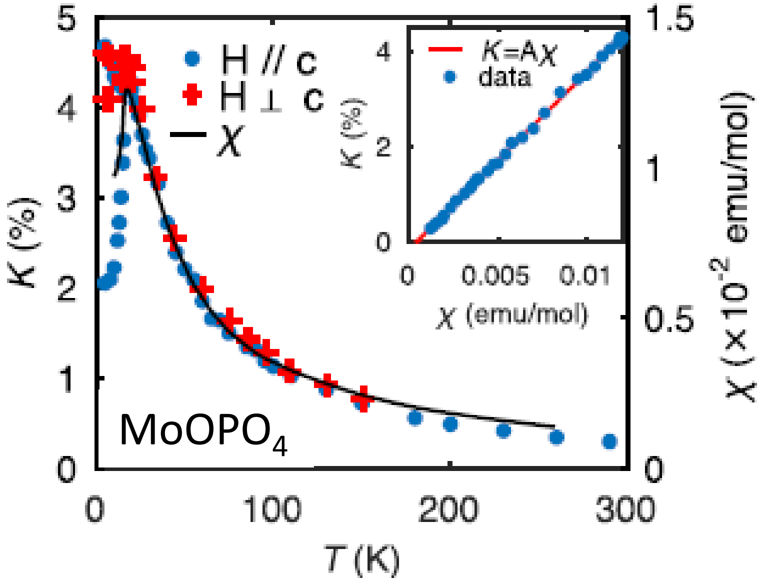

REFERENCE

DIAMAGNETS

chemical shift
T-independent

PARAMAGNETS

Knight shift
T-dependent

$$K \sim \chi$$

FERROMAGNETS

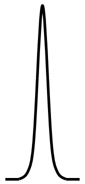

presence of an internal field, possible even with $B_0 = 0$

Phys.Rev. 140, A854 (1965)

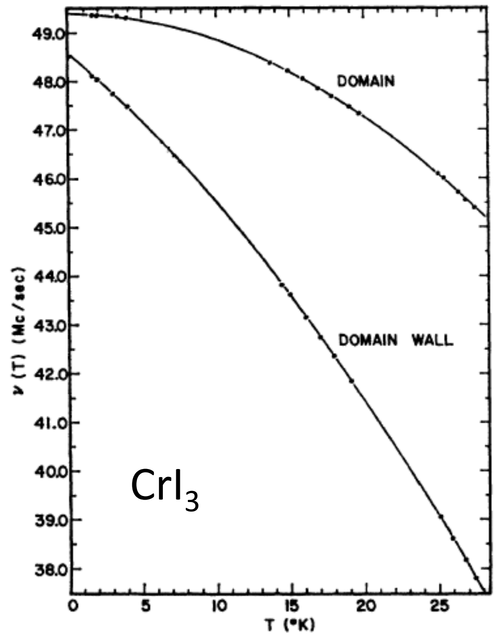

PARAMAGNETS

ANTIFERROMAGNETS

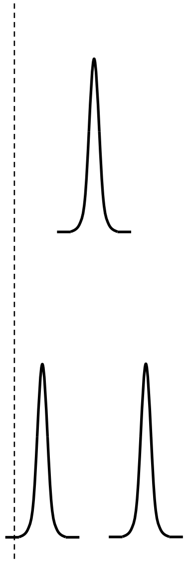

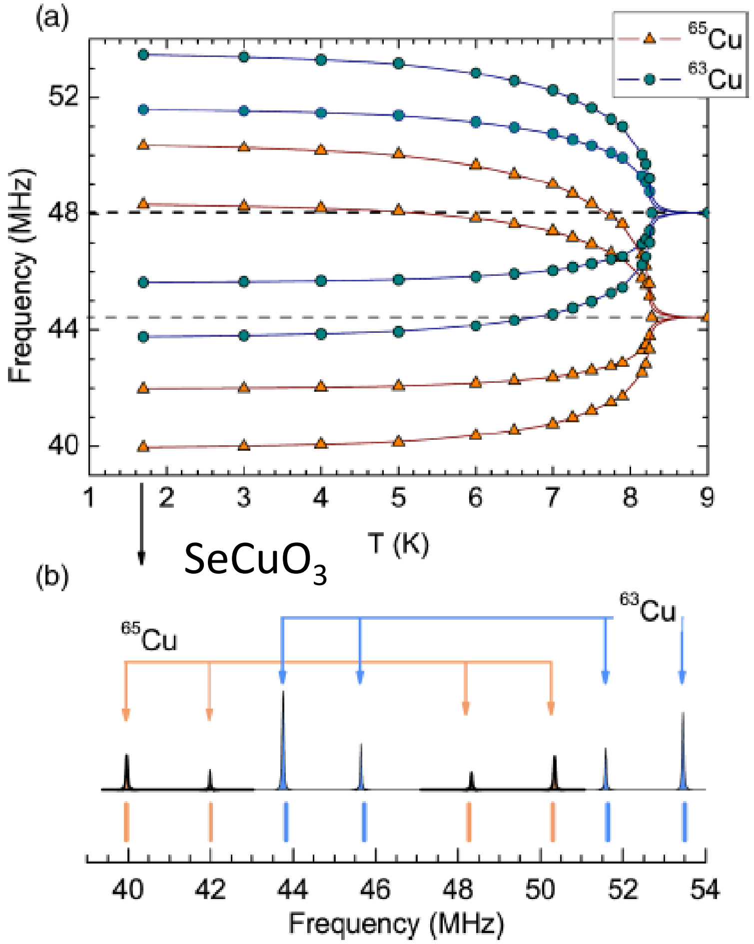

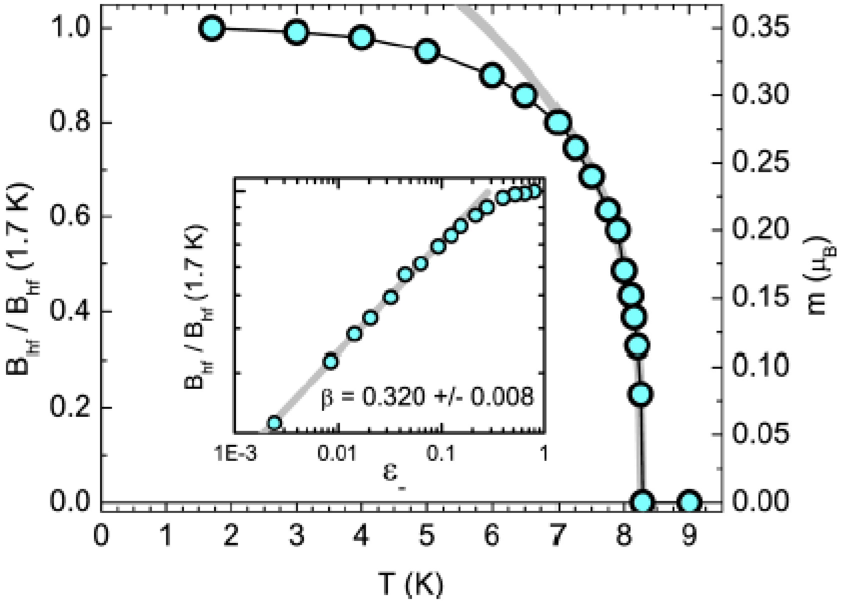

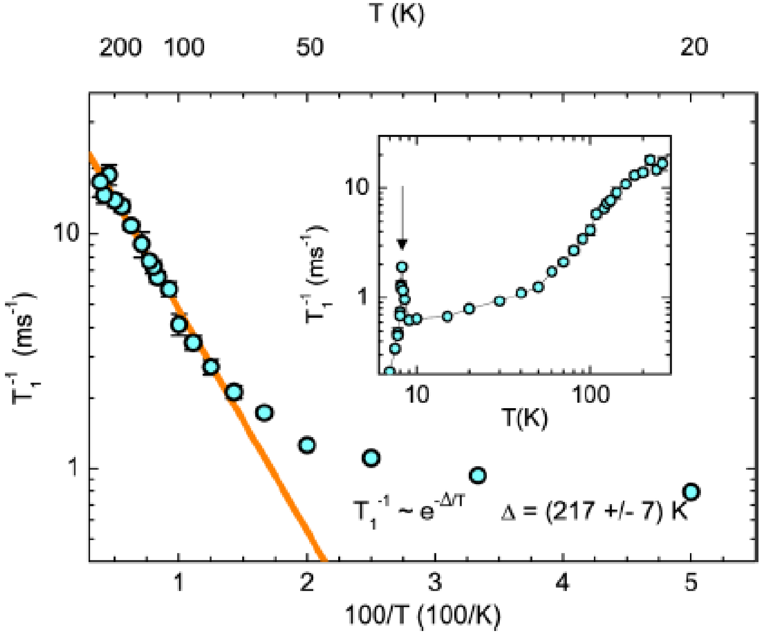

REFERENCE

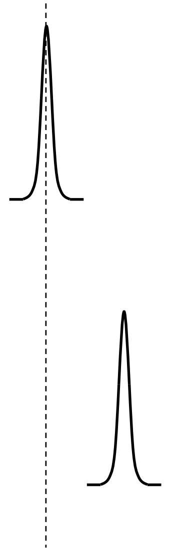

METALS

Knight shift
T-independent

$$K = \frac{A_{hf}}{\hbar^2 \gamma_e \gamma_n} \chi_P = \frac{A_{hf} \gamma_e}{2\gamma_n} n(E_F)$$

SC gap

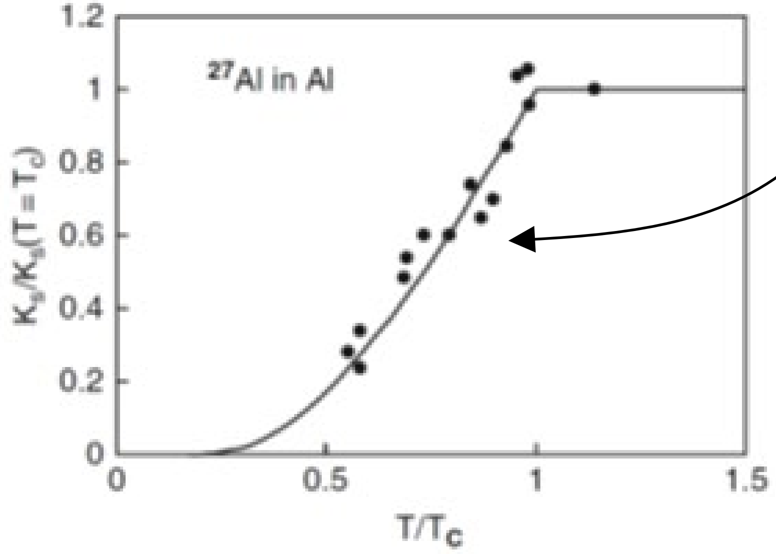

REFERENCE

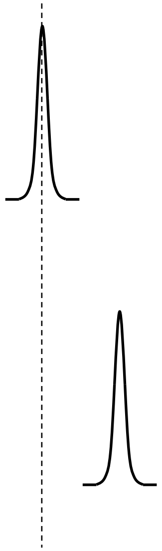

METALS

Knight shift
T-independent

$$K = \frac{A_{hf}}{\hbar^2 \gamma_e \gamma_n} \chi_P = \frac{A_{hf}\gamma_e}{2\gamma_n} n(E_F)$$

$$\frac{1}{T_1 T K^2} = \frac{4\pi k_B}{\hbar}\left(\frac{\gamma_n}{\gamma_e}\right)^2$$

Korringa relation (Fermi liquid)

deviations for correlated metals

Nature 434, 622 (2005)

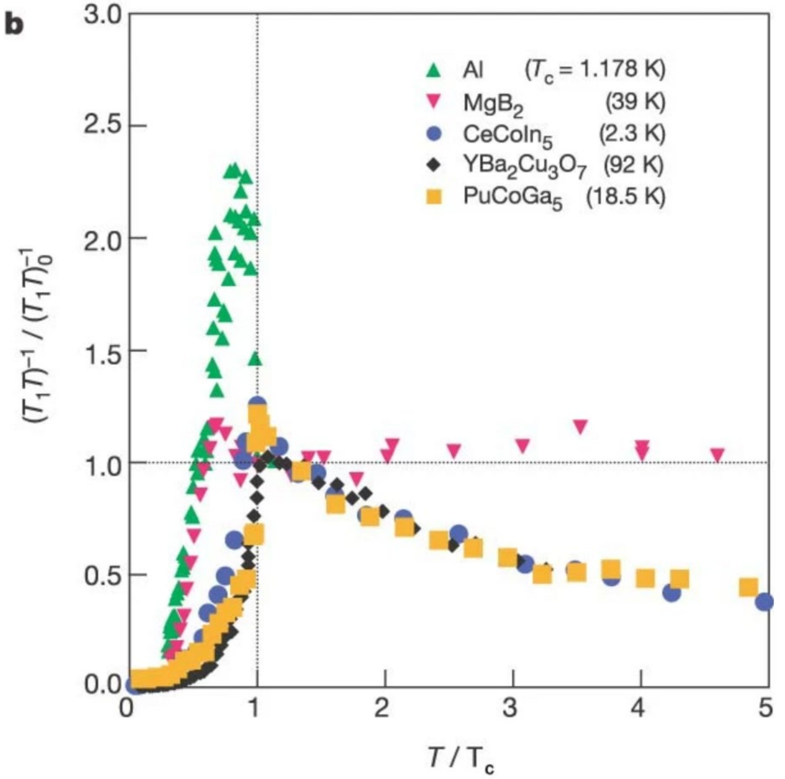

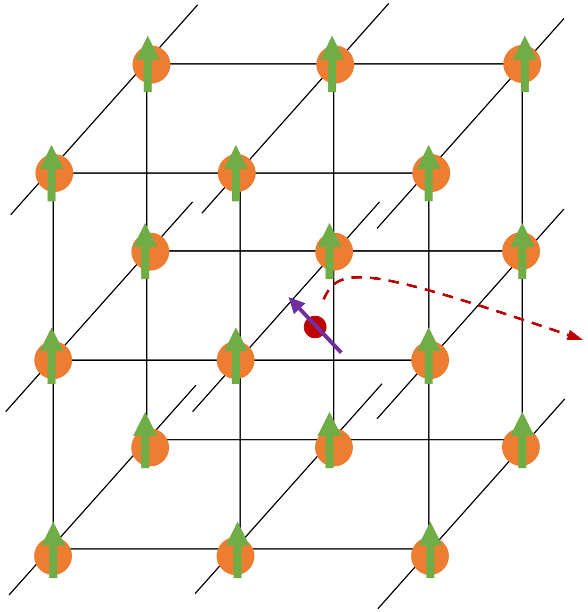

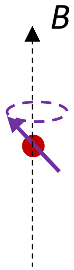

precession due to a *local* magnetic field

muon spin <u>rotation</u>

$B \gtrsim 0.1$ G $\quad \mu \gtrsim 0.001\, \mu_B$

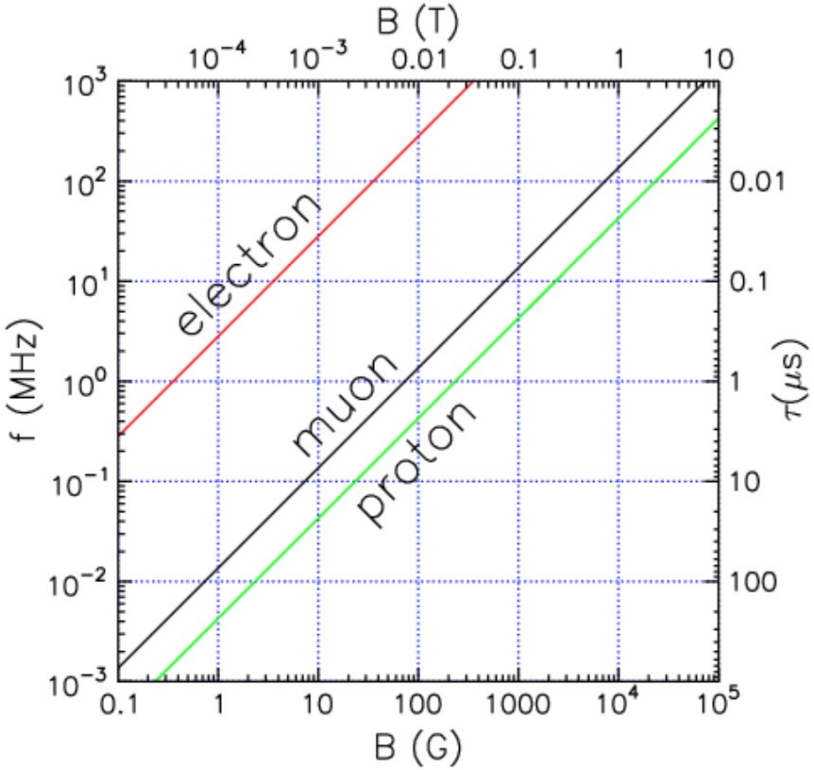

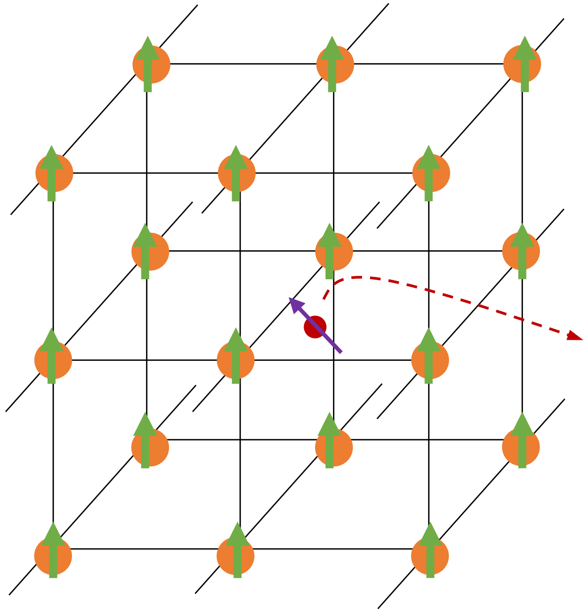

interstitial

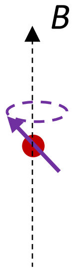

$B \gtrsim 0.1\ \mathrm{G} \qquad \mu \gtrsim 0.001\ \mu_B$

precession due to a *local* magnetic field

muon spin rotation

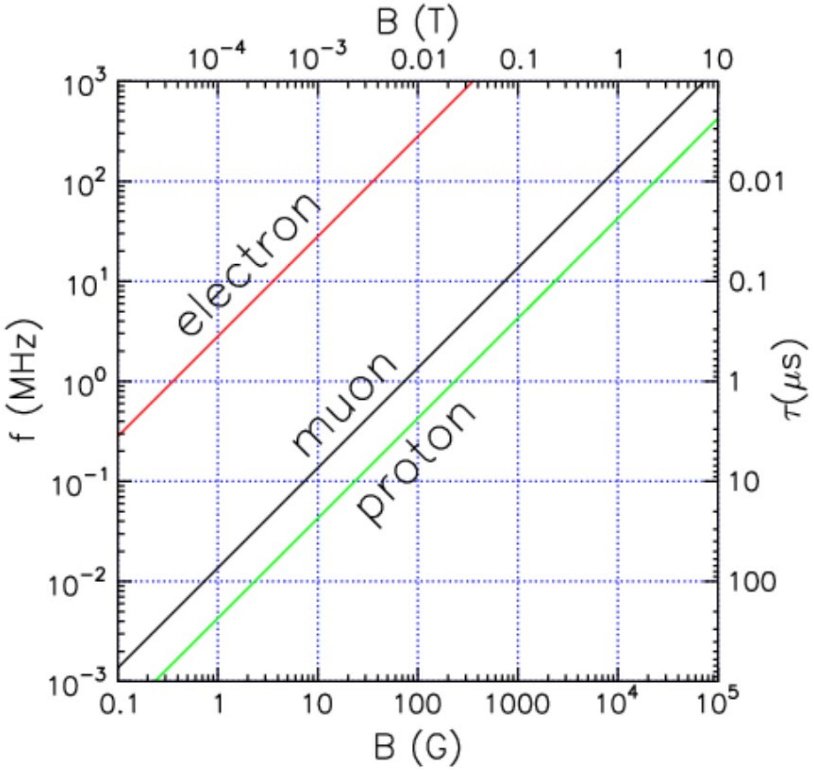

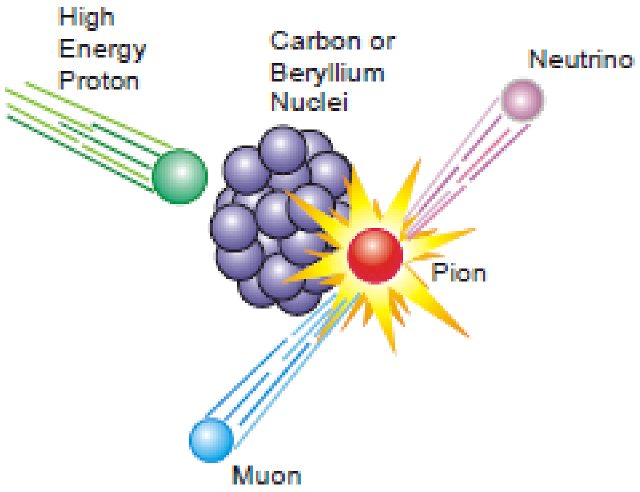

$$p + p \rightarrow p + n + \pi^+$$

$$p + n \rightarrow n + n + \pi^+$$

$$\pi^+ \xrightarrow{26ns} \mu^+ + \nu_\mu$$

spin antiparallel to momentum

$\xrightarrow{\text{thermalization}}$

$$\mu^+ \xrightarrow{2.2\mu s} e^+ + \nu_e + \overline{\nu_\mu}$$

image source: wikimedia.org

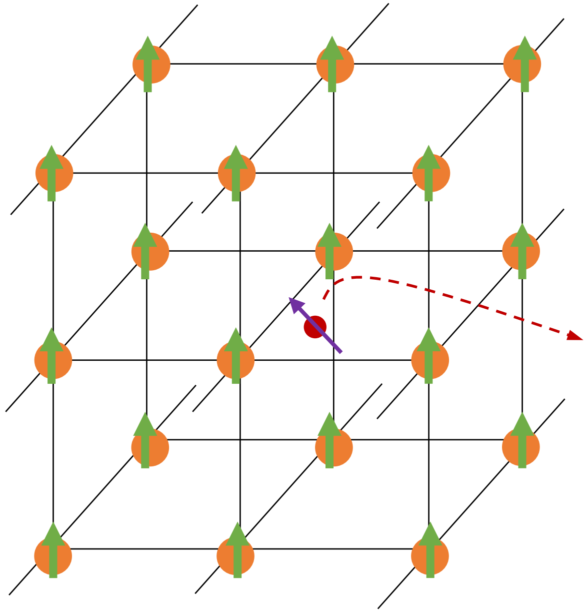

interstitial

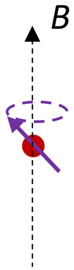

$B \gtrsim 0.1\ \mathrm{G}$ $\quad \mu \gtrsim 0.001\ \mu_B$

precession due to a *local* magnetic field

muon spin rotation

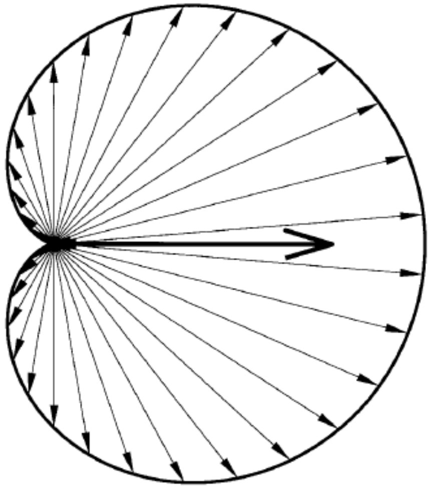

preferably in the direction of the muon spin

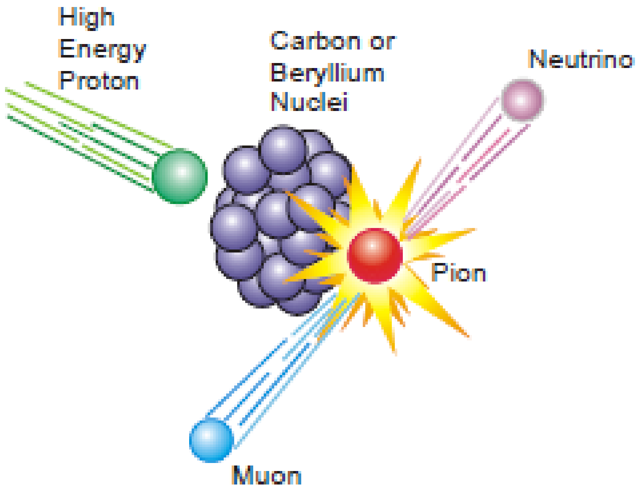

$$p + p \rightarrow p + n + \pi^+$$

$$p + n \rightarrow n + n + \pi^+$$

$$\pi^+ \xrightarrow{26ns} \boxed{\mu^+ + \nu_\mu}$$

spin antiparallel to momentum

$\xRightarrow{\text{thermalization}}$

$$\mu^+ \xrightarrow{2.2\mu s} e^+ + \nu_e + \overline{\nu_\mu}$$

image source: wikimedia.org

❖ μSR facilities

International Society for μSR Spectroscopy

HOME | Muon Links | Communications | Logistics | Forum | CONTACT

Muon facilities

- TRIUMF CMMS (Centre for Molecular & Materials Science
- PSI LMU/SμS (Laboratory for Muon Spin Spectroscopy/Swiss Muon Source)
- ISIS Muons & RIKEN-RAL Muon Facility
- J-PARC MLF (Materials & Life Sciences Facility)
- MuSIC (DC Muon Reseach Group, RCNP)
- Project EMuS (Experimental Muon Source) at the Chinese Spallation Neutron Source CSNS (pulsed)
- Project Muon Facility at the South Korean RAON (Rare Isotope Science Project) (DC)

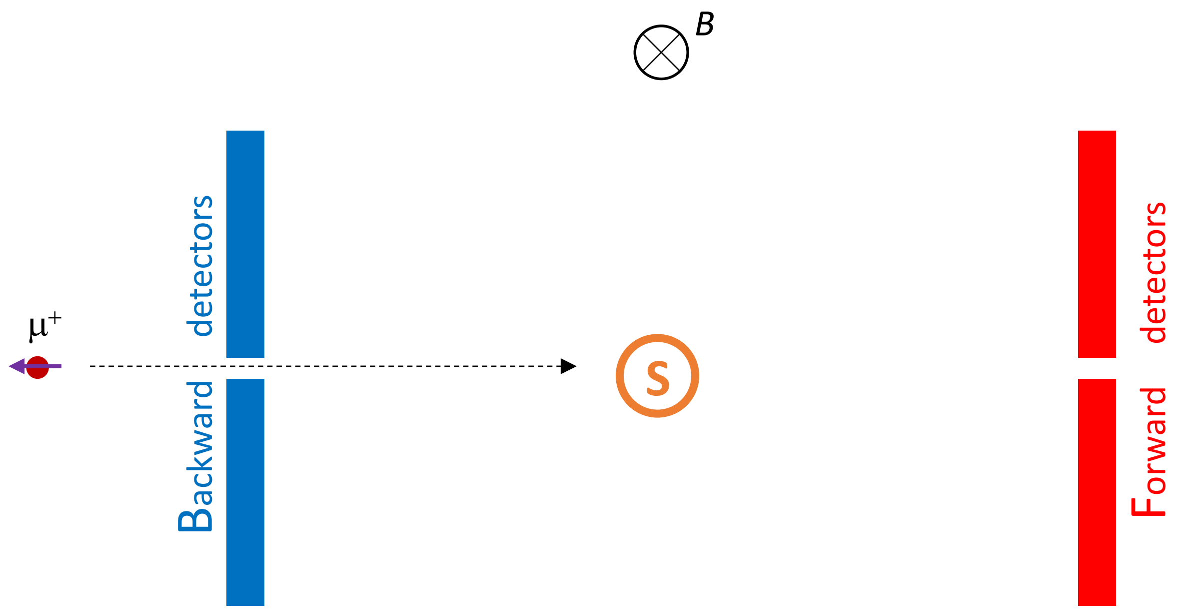
B
μ+
Backward detectors
S
Forward detectors

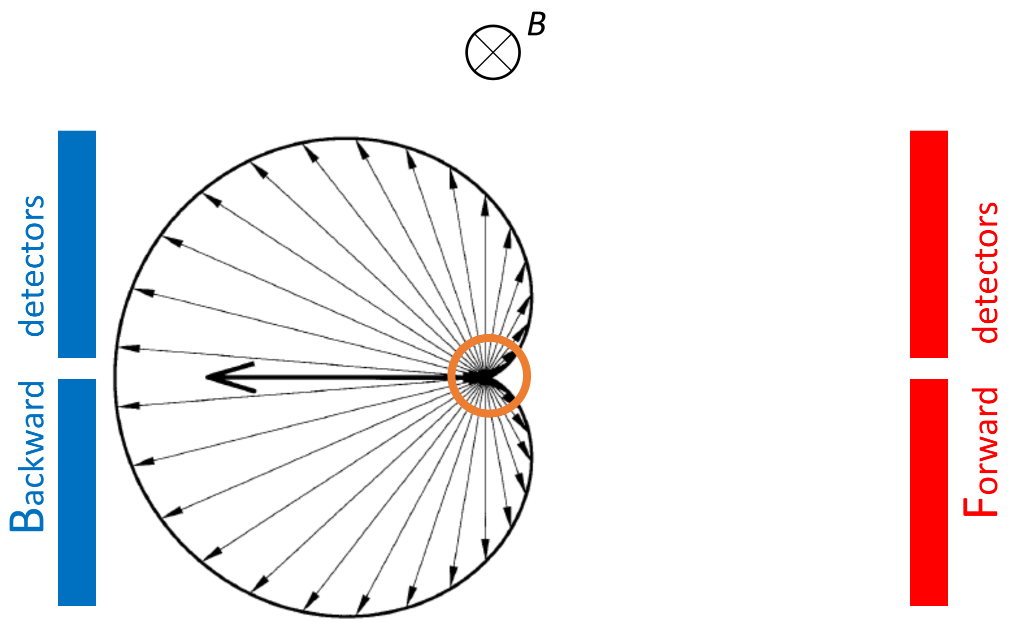
B
Backward detectors
Forward detectors

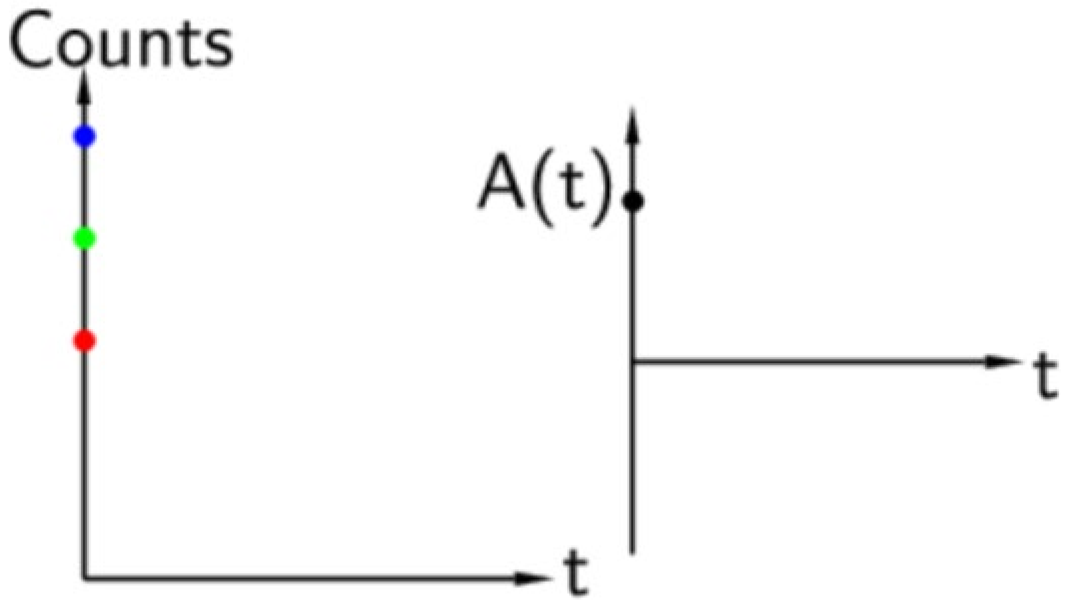
Counts
t
A(t)
t

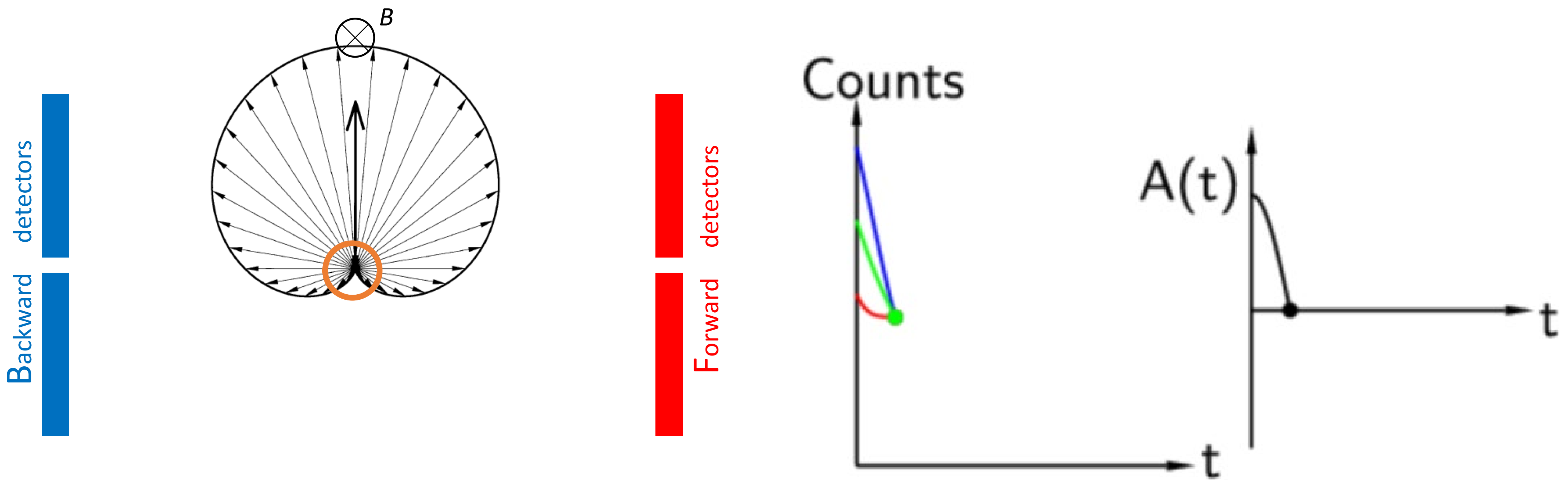
B
Backward detectors
Forward detectors
Counts
t
A(t)
t

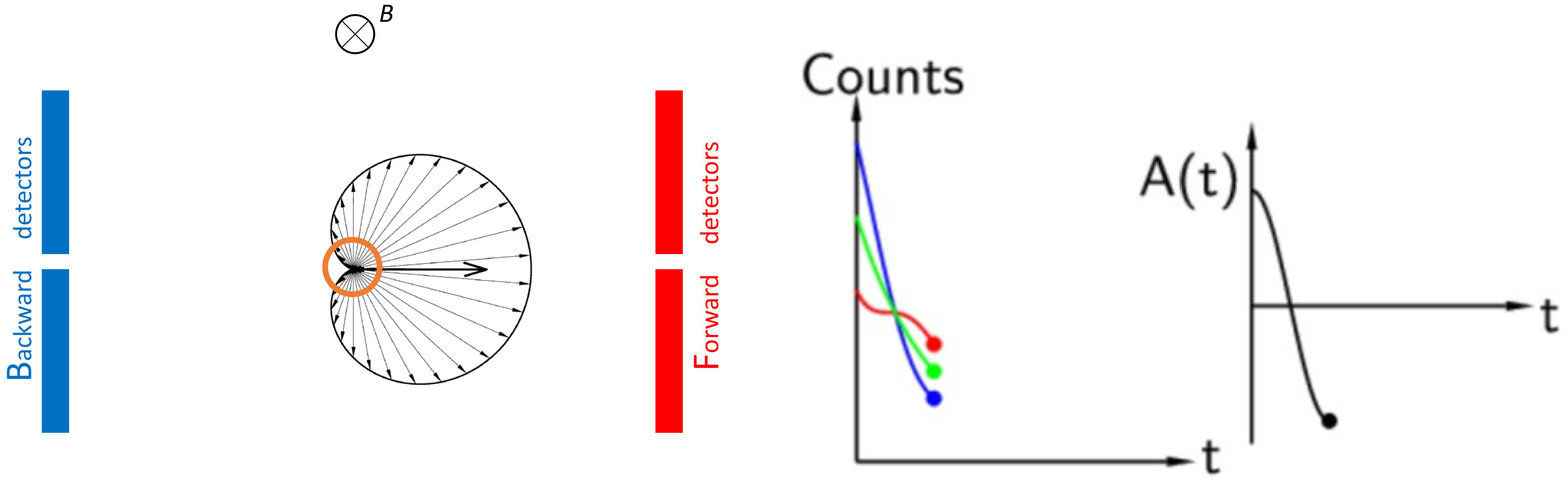
B
Backward detectors
Forward detectors
Counts
t
A(t)
t

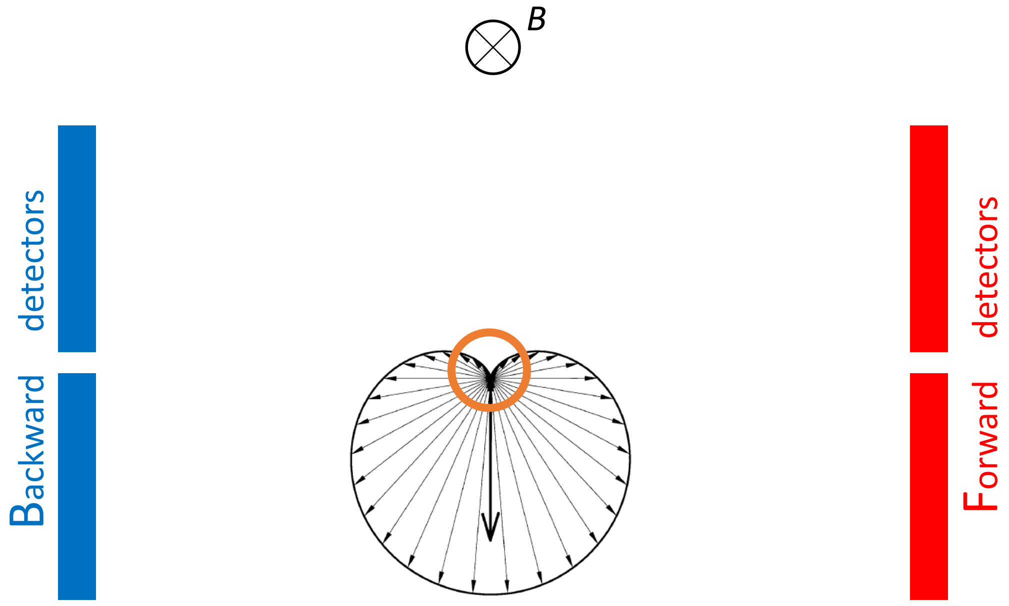
B
Backward detectors
Forward detectors

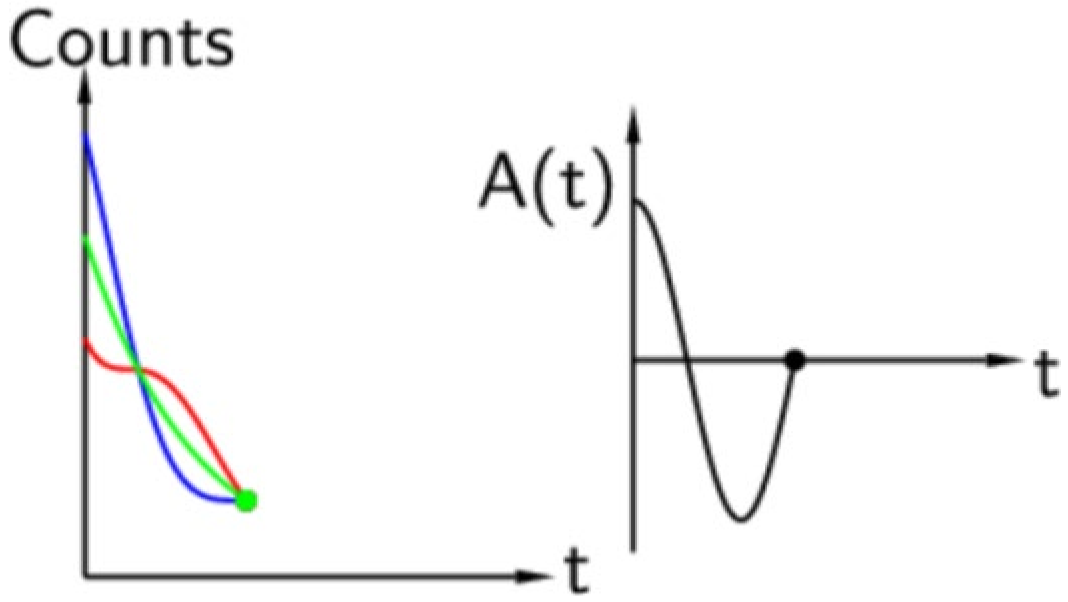
Counts
t
A(t)
t

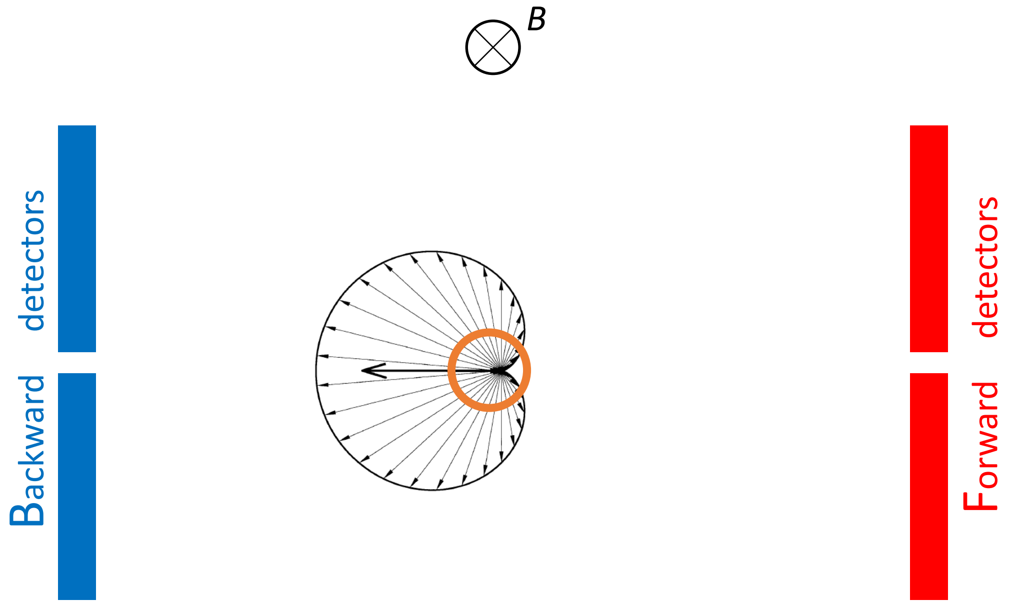
B
Backward detectors
Forward detectors

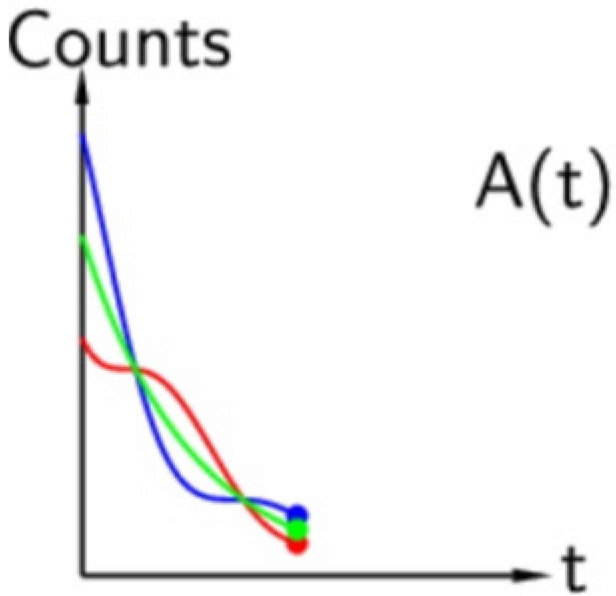
Counts
t

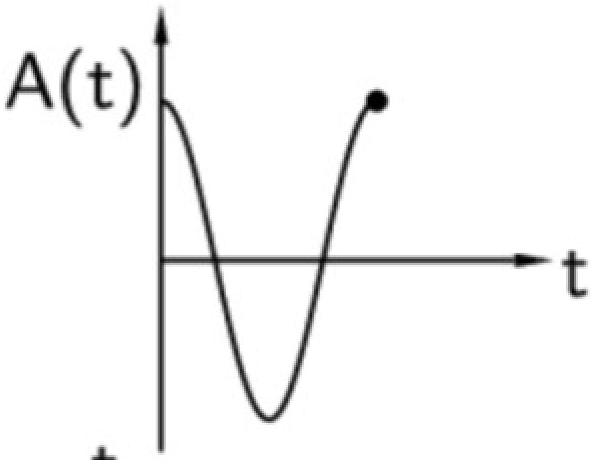
A(t)
t

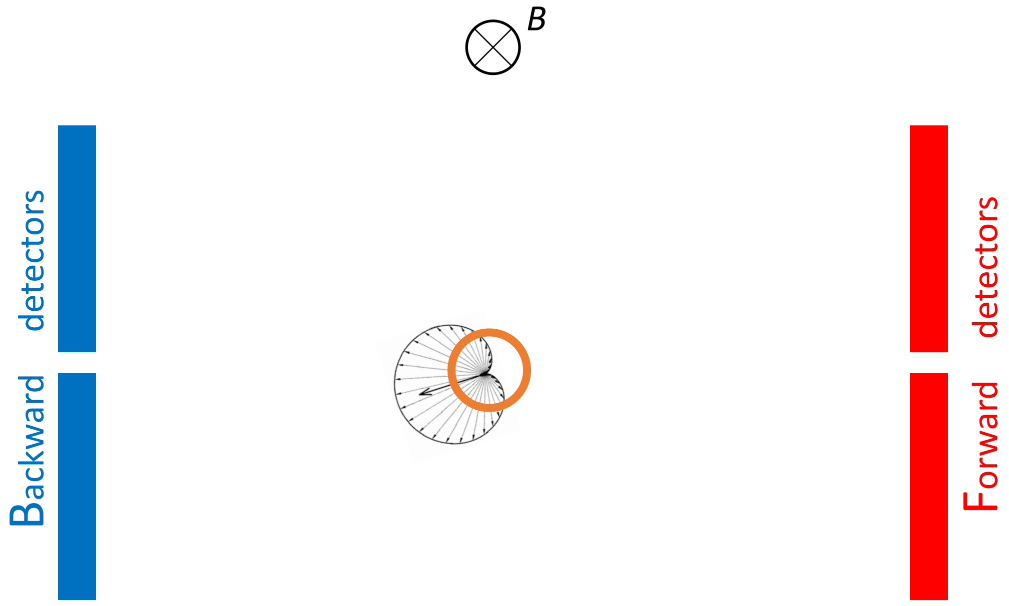

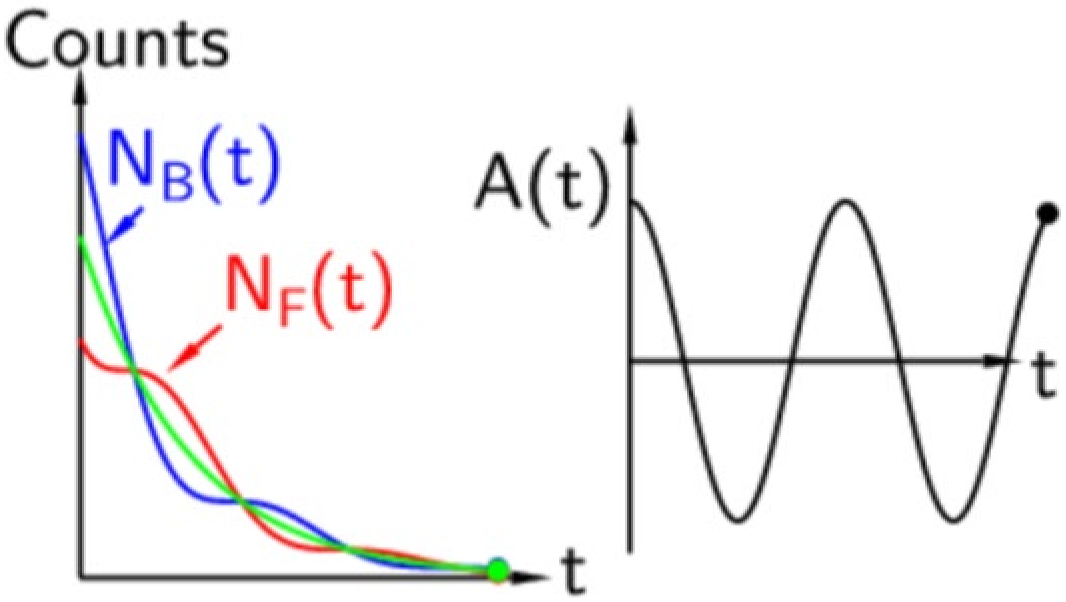

$$A(t) = \frac{N_B(t) - N_F(t)}{N_B(t) + N_F(t)}$$

asymmetry function

$$A(t) = \frac{N_B(t) - N_F(t)}{N_B(t) + N_F(t)}$$

$$\mathrm{G}(t) = A(t)/A_{max}$$

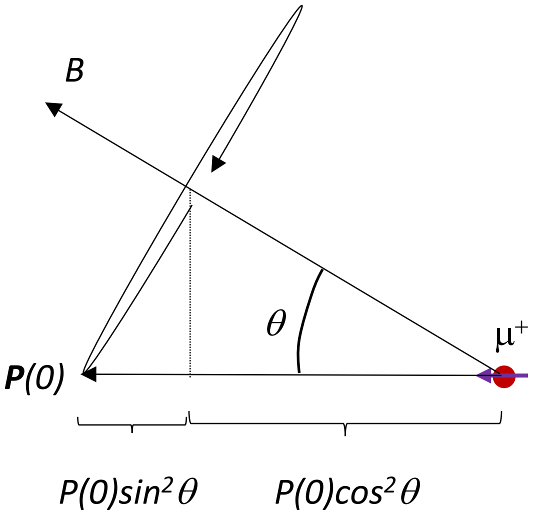

$$\mathrm{G}(t) = (\cos\theta)^2 + (\sin\theta)^2 \cos\omega t \qquad \omega = \gamma_\mu B$$

$$A(t) = \frac{N_B(t) - N_F(t)}{N_B(t) + N_F(t)}$$

$$\mathrm{G}(t) = A(t)/A_{max}$$

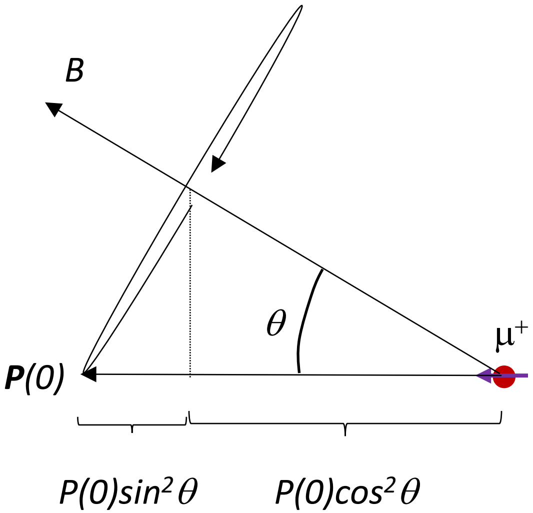

$$\mathrm{G}(t) = (\cos\theta)^2 + (\sin\theta)^2 \cos\omega t \qquad \omega = \gamma_\mu B$$

random field orientation
integration over a sphere

$$\mathrm{G}(t) = \frac{1}{3} + \frac{2}{3}\cos\omega t$$

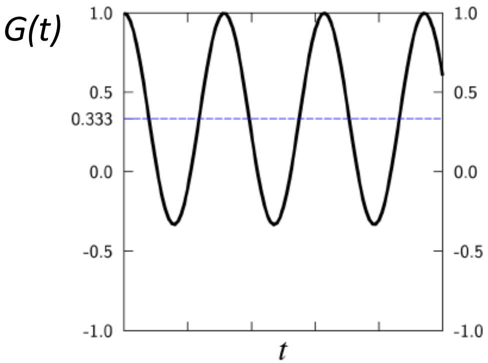

$$A(t) = \frac{N_B(t) - N_F(t)}{N_B(t) + N_F(t)}$$

$$\mathrm{G}(t) = A(t)/A_{max}$$

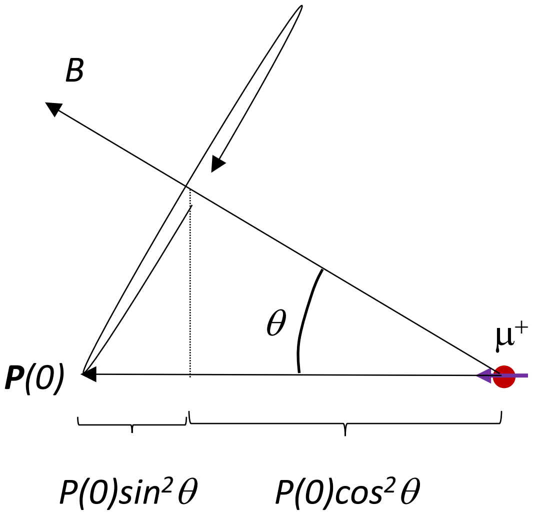

Gaussian distribution

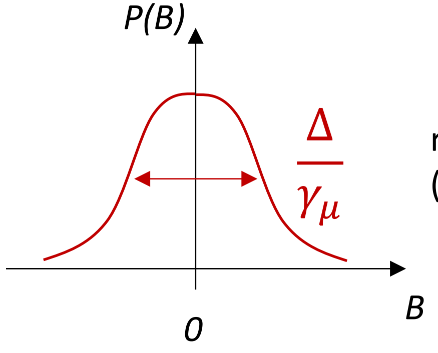

randomly oriented nuclear spins
(static within the μSR time window)

$$\mathrm{G}(t) = (\cos\theta)^2 + (\sin\theta)^2 \cos\omega t \qquad \omega = \gamma_\mu B$$

$$\mathrm{G}(t) = \frac{1}{3} + \frac{2}{3}(1 - \Delta^2 t^2)e^{-\frac{\Delta^2 t^2}{2}}$$

random field orientation
integration over a sphere

$$\mathrm{G}(t) = \frac{1}{3} + \frac{2}{3}\cos\omega t$$

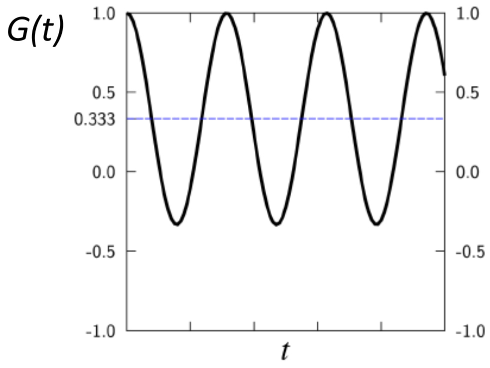

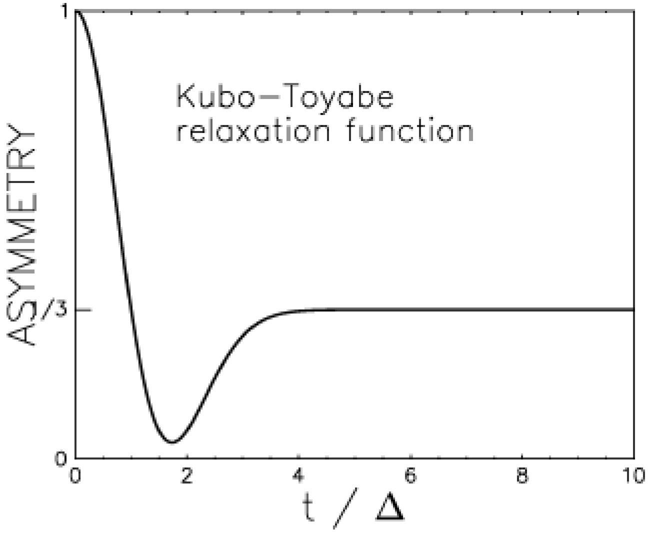

$$A(t) = \frac{N_B(t) - N_F(t)}{N_B(t) + N_F(t)}$$

$$G(t) = A(t)/A_{max}$$

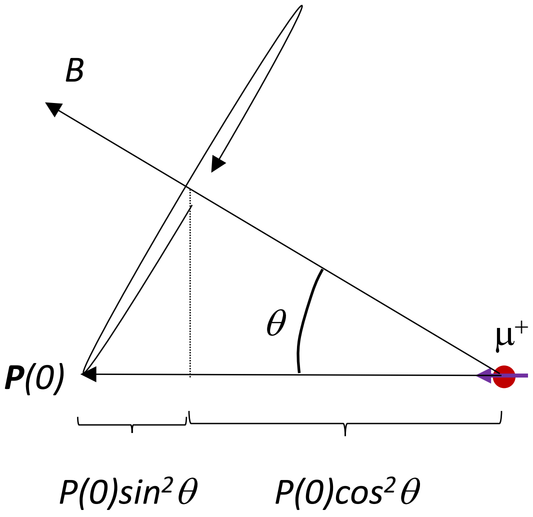

Gaussian distribution

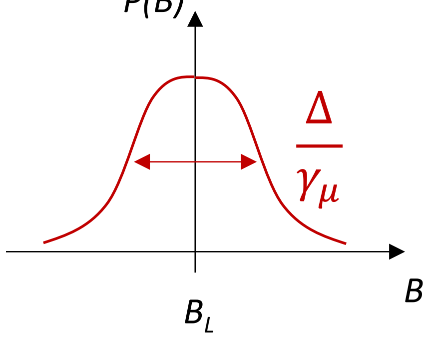

$$G(t) = (\cos\theta)^2 + (\sin\theta)^2 \cos\omega t \qquad \omega = \gamma_\mu B$$

random field orientation

integration over a sphere

$$G(t) = \frac{1}{3} + \frac{2}{3}\cos\omega t$$

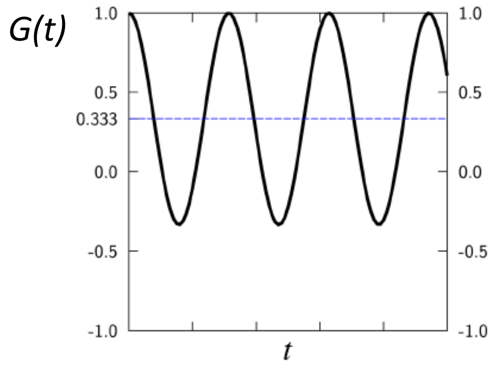

External magnetic field

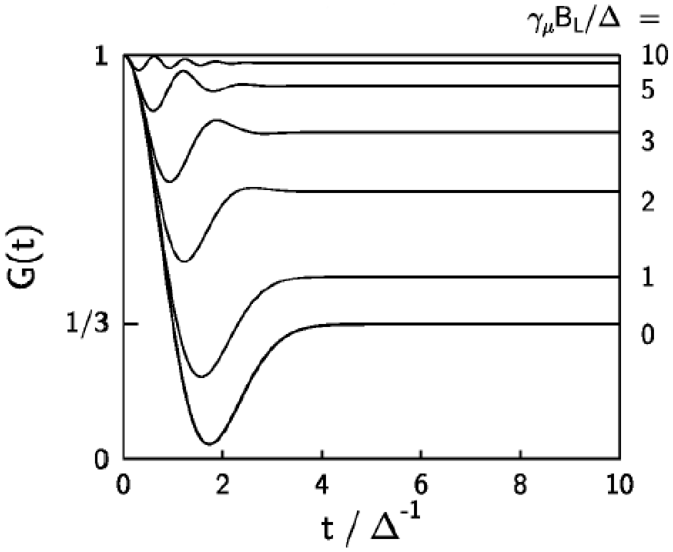

JPSJ 49, 1773 (1980)

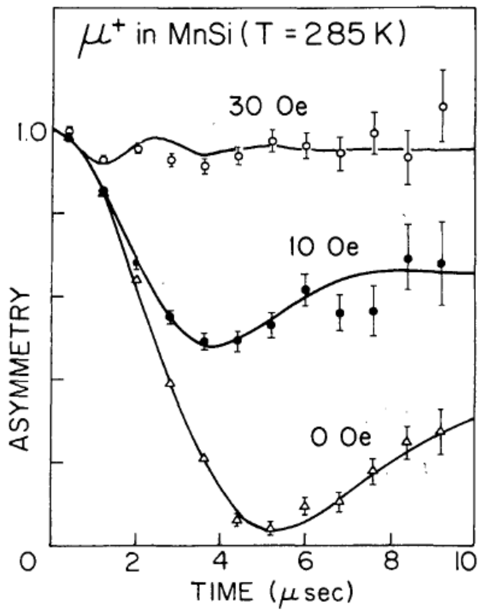

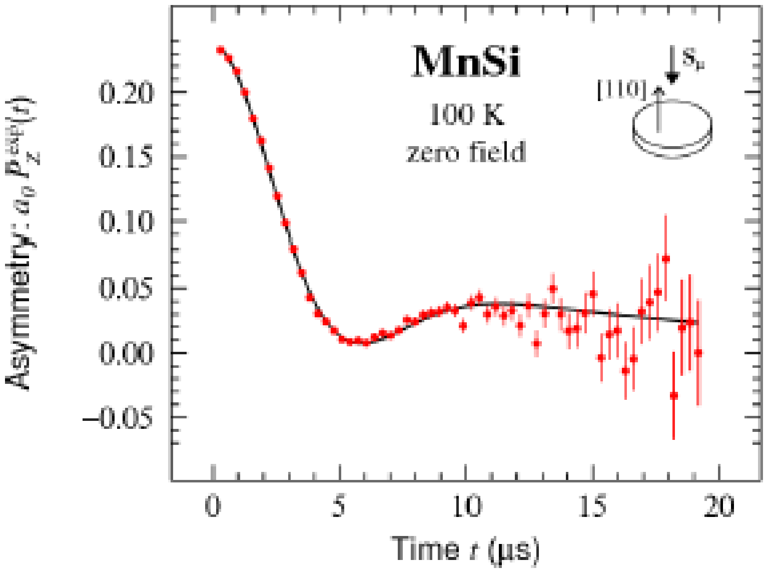

$$G(t) = e^{-\lambda t} G_{KT}(t)$$

electronic

nuclear

time-dependence of internal fields (fluctuations, μ-diffusion)

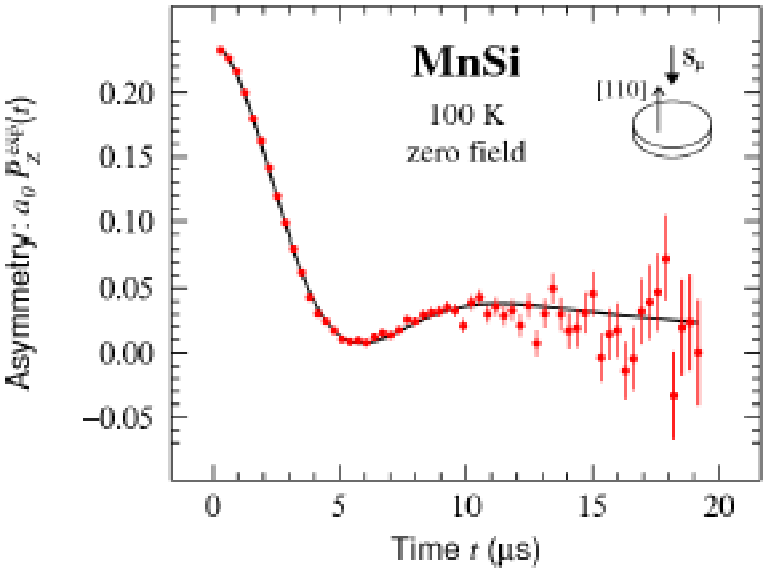

$$G(t) = e^{-\lambda t} G_{KT}(t)$$

electronic

nuclear

time-dependence of internal fields (fluctuations, μ-diffusion)

magnetic order

PRL 98, 197203 (2007)

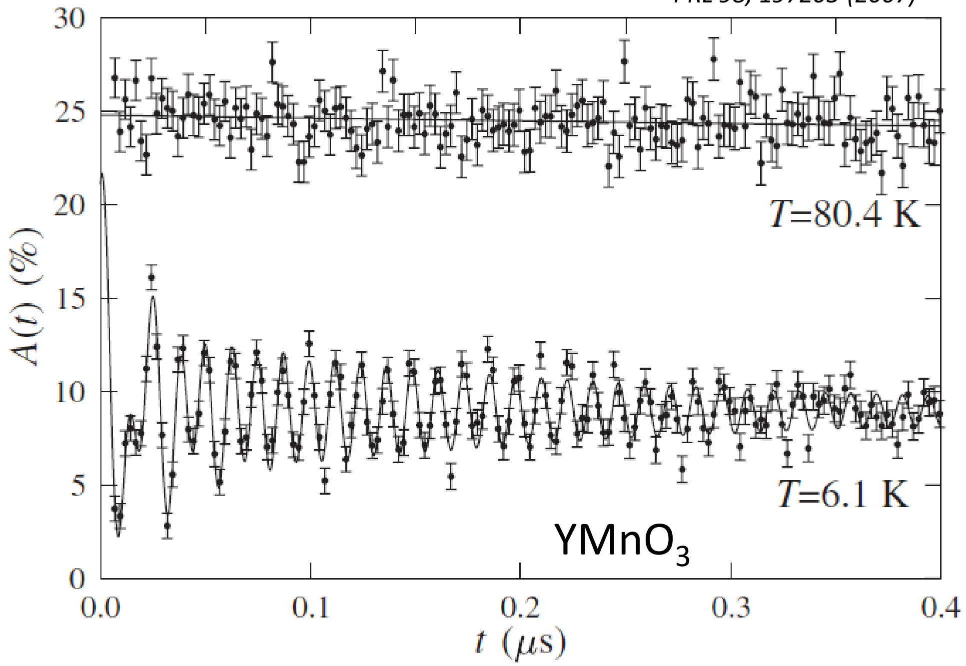

magnetic order

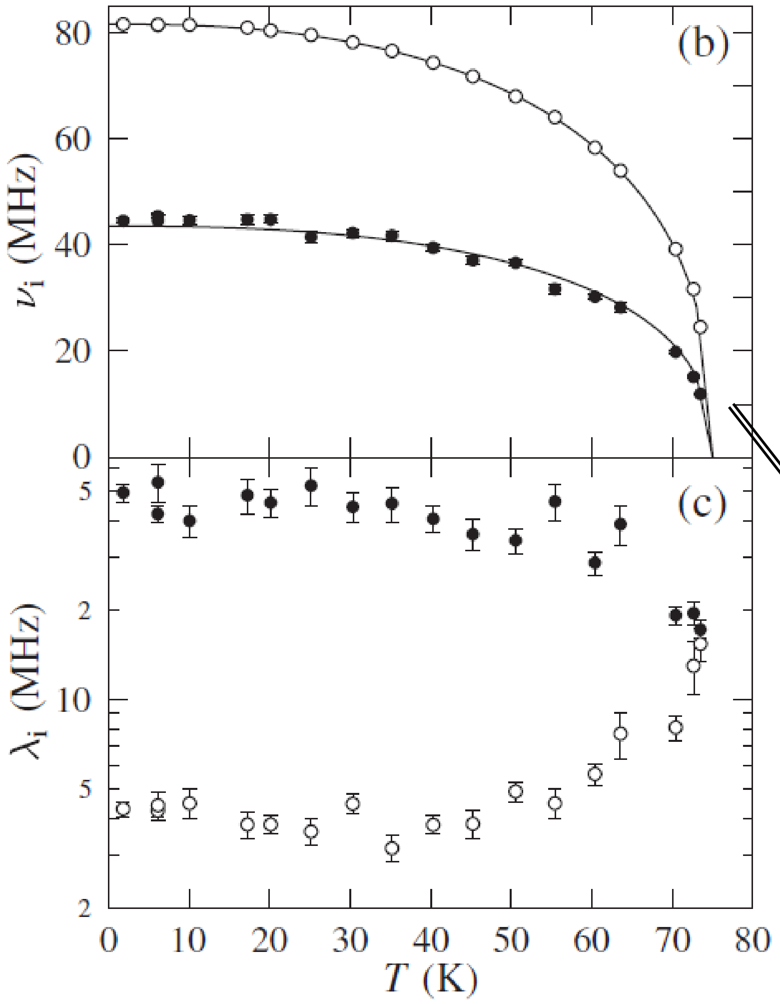

PRL 98, 197203 (2007)

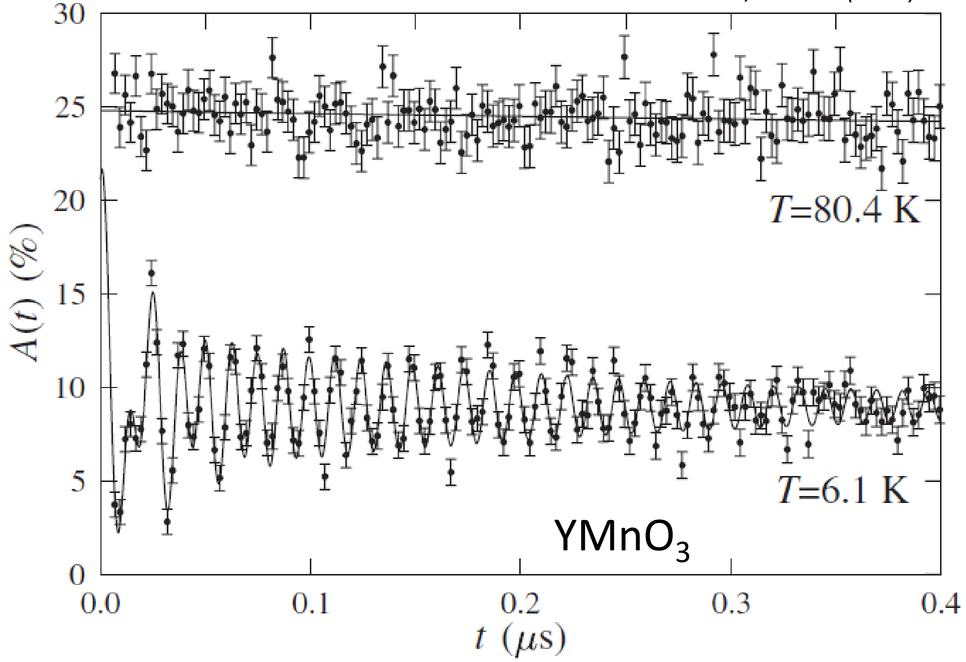

- two muon stopping sites....but where exactly?
- typically 1 Å from oxygen (DFT)
- reverse-engineering the structure from dipole fields (~10^5 sites)

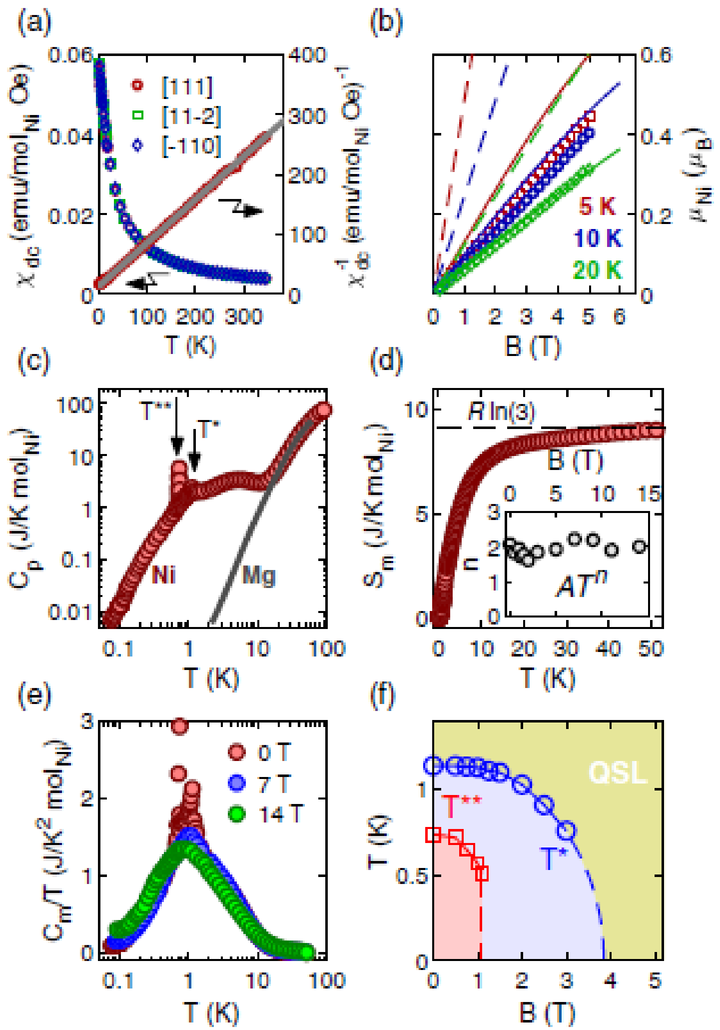
(a)
(b)
[111]
[11-2]
[-110]
T (K)
B (T)
5 K
10 K
20 K
(c)
(d)
T**
T*
Ni
Mg
R ln(3)
AT^n
T (K)
(e)
(f)
0 T
7 T
14 T
QSL
T**
T*
T (K)
B (T)

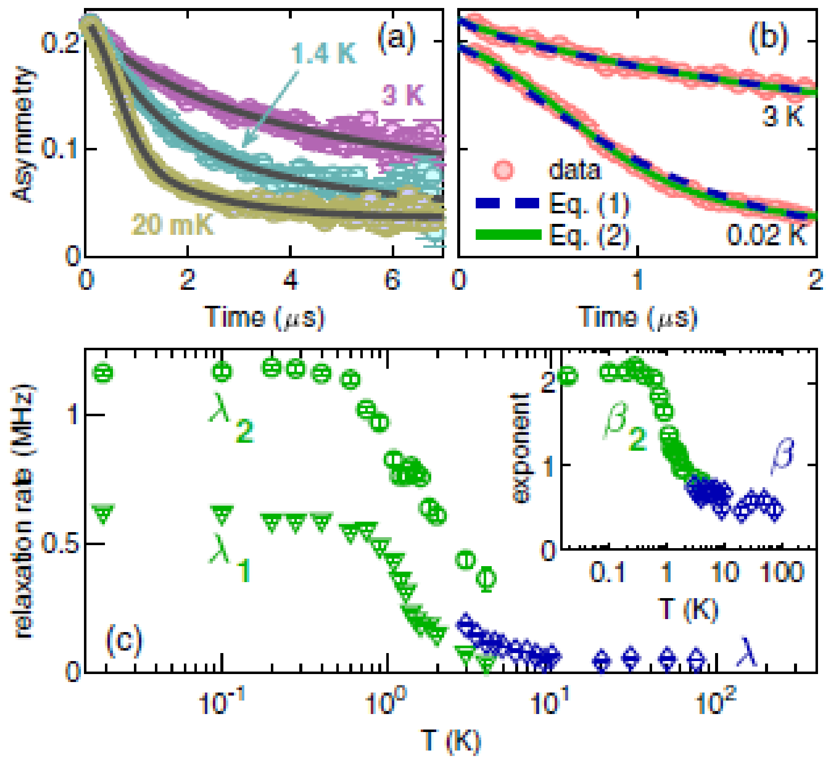
(a)
(b)
Asymmetry
1.4 K
3 K
20 mK
data
Eq. (1)
Eq. (2)
3 K
0.02 K
Time (μs)
(c)
relaxation rate (MHz)
exponent
T (K)

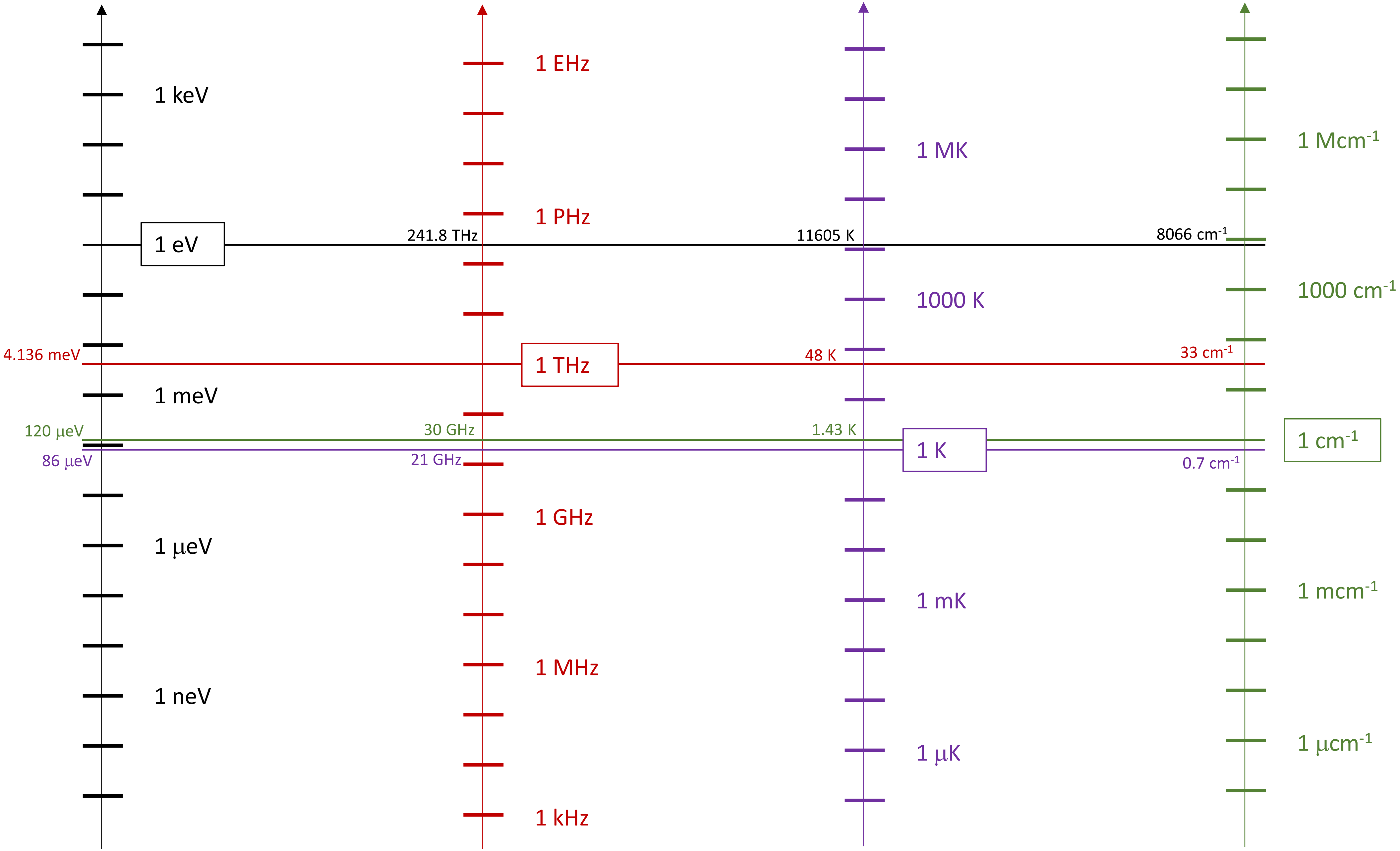
1 keV
1 eV
1 meV
1 μeV
1 neV
1 EHz
1 PHz
1 THz
1 GHz
1 MHz
1 kHz
1 MK
1000 K
1 K
1 mK
1 μK
1 Mcm-1
1000 cm-1
1 cm-1
1 mcm-1
1 μcm-1
241.8 THz
11605 K
8066 cm-1
4.136 meV
48 K
33 cm-1
120 μeV
30 GHz
1.43 K
86 μeV
21 GHz
0.7 cm-1